46TH TURBOMACHINERY & 33RD PUMP SYMPOSIA
HOUSTON, TEXAS | DECEMBER 11-14, 2017
GEORGE R. BROWN CONVENTION CENTER

A MORE COMPREHENSIVE EVALUATION OF EQUATION OF STATE INFLUENCES ON COMPRESSOR PERFORMANCE DETERMINATION

Mark R. Sandberg, P.E.
Principal Consulting Engineer
Sandberg Turbomachinery Consulting, LLC
Montgomery, Texas, USA

Mark R. Sandberg is the principal of Sandberg Turbomachinery Consulting, LLC. Before forming this consulting practice in 2016, he was a Consulting Machinery Engineer with Chevron Energy Technology Company in Houston, Texas for more than fifteen years. Prior to joining Chevron, he was employed by ARCO, Petro-Marine Engineering, and The Dow Chemical Company. During his sixteen years at ARCO, he was involved with a number of gas turbine driven compressors, both internationally and on the North Slope of Alaska. Throughout the majority of his career, he has been involved in providing technical assistance and services associated with the selection, design, specification, procurement, and testing of new rotating equipment along with failure analysis and troubleshooting issues with existing equipment, primarily in upstream oil and gas production and LNG processing operations. Mark has more than 40 years of varied experience in the process industries and has been involved with the design, manufacture, testing, and installation of several small to large gas turbine driven centrifugal compressor trains worldwide. Mr. Sandberg has B.S.M.E. and M.S. (Mechanical Engineering) degrees from the University of Illinois at Urbana-Champaign, is a registered Professional Engineer in the State of Texas, an Emeritus Member of the Texas A&M Turbomachinery Advisory Committee, a member of AIAA and a Fellow Member of ASME.

ABSTRACT

A previous paper by the author, Sandberg (2005), addressed the impacts of using a number of different equations of state to calculate compressor performance parameters. These were compared against one another with equipment supplier values utilized as the baseline. Additional analyses were completed to provide a more accurate and alternate comparison of equation of state accuracy through the use of experimental PVT (pressure-volume-temperature) data. This was done by comparing different equation of state estimates of compressibility factor against the PVT data for a number of data sets found in publicly available literature. Several more recent databases have become available in the literature that extend PVT data to higher pressures. This is valuable as compression applications are appearing that have design operating pressures above previous limits. The introduction of a relatively new equation of state, GERG, is also claimed to be a more accurate equation of state when compared against other, more commonly used for compression applications.

This investigation will address and provide relevant information on the following topics:

1. Provide an expanded evaluation and comparison between a number of commonly utilized equations of state and PVT data available in the open literature for a number of different gases and gas mixtures. The results of this analysis will identify those equations of state that provide superior accuracy in the prediction of real gas densities and compressibility factors across a range of pressures and temperatures normally encountered in compression applications.
2. Introduce and describe a novel method to derive empirical departure enthalpy and entropy estimates from PVT data, effectively allowing a comparison between predicted and derived actual values of the departure functions. This will allow additional evaluation of relative accuracies of predicted values of efficiencies and powers from the different equations of state.
3. Present a comparison of calculated compressor performance parameters (including polytropic head, efficiency, work input and specific gas power) for a range of typical compressor applications using the different equations of state examined. Specific recommendations for the most accurate equations of state for different gases and operating conditions will also be included.

INTRODUCTION

The successful evaluation of compressor aero-thermodynamic performance is dependent upon only a few operating parameters. Accurate measurements of total pressure and temperature at the compressor inlet and discharge nozzles along with an accurate gas composition are the primary variables needed, however, it is assumed that the thermophysical properties derived from these measurements are equally as accurate. Unfortunately, this is not always the case. ASME PTC 10 Type II (1997) tests are normally carried out at relatively low pressure levels where the primarily inert gases have thermophysical properties near ideal gas conditions. Alternatively, ASME PTC 10 Type I tests and any field testing performed under actual operating conditions might occur with gas properties considerably different from ideal gas conditions. In these cases, thermophysical properties must be estimated from some form of a real gas equation of state which takes into account the non-ideal behavior of the compressed fluid.

A relatively large number of generalized and compositional equations of state exist which may be utilized to calculate real gas thermophysical properties. While a few sources exist providing recommendations regarding the most accurate application of an equation of state for a specific range of gas compositions, there is little supporting information addressing the degree of accuracy in the application of these equations of state. This may create the need for the equipment manufacturer, engineering contractor, and end-user to have a discussion regarding the most appropriate equation of state to be used for compressor performance prediction and evaluation. Optimally, such a discussion should take place prior to the order placement and design of the compression equipment. At times, it may not occur at all, leaving the equipment supplier to select the utilized equation of state for thermophysical properties prediction. Additionally, the simulation and design of the associated process facilities including the compression equipment may utilize a different equation of state. Depending upon relative property prediction accuracy, this may result in differences in predicted and actual compression performance parameters and associated power requirements between the equipment supplier and process designers.

The severity of compression applications has continually evolved with increasingly higher discharge pressures and compositions of the handled gases. This is particularly the case with reinjection compression applications where discharge pressures have increased well into the dense phase region of the fluid phase envelope. The dense phase region is characterized by gas properties that reflect both gas and liquid properties. Figure 1 is a photo of the Kashagan sour gas reinjection compressor train. It has been publicized as completing the highest pressure full load, full pressure factory acceptance test on record, with a discharge pressure during test reaching nearly 12,000 psig (820 barg).

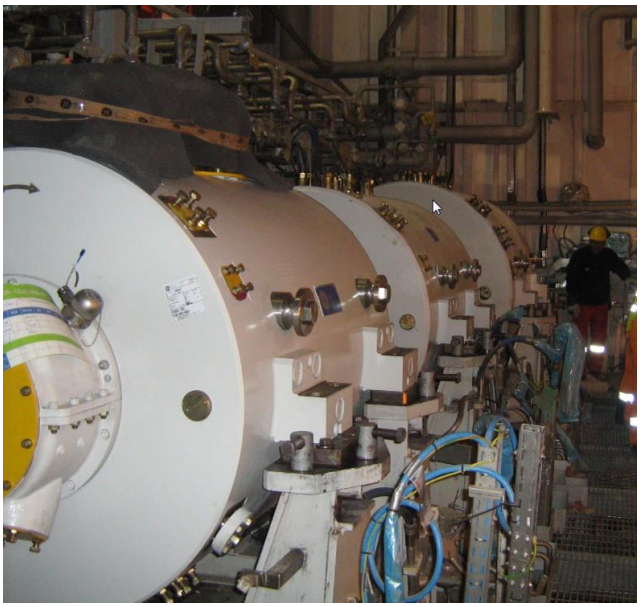

Photo Courtesy of GE Oil & Gas

Figure 1: Kashagan Reinjection Compressor Train

While compressor discharge pressure is certainly a critical parameter in compressor design and operation, it is not the only parameter that impacts mechanical, rotordynamic, and aero-thermodynamic design considerations. Another critical parameter is the density of the fluid being handled. The publicized record of high density belongs to the reinjection machines for the Tupi III Project. Although the discharge pressure attained during factory acceptance testing was below that of the Kashagan Project, the high carbon dioxide concentration of the gas resulted in a higher discharge density which was reportedly equivalent to that of a natural gas mixture at approximately 13,000 psig (900 barg). Figure 2 is a photograph of the Tupi III compressor on the factory test stand.

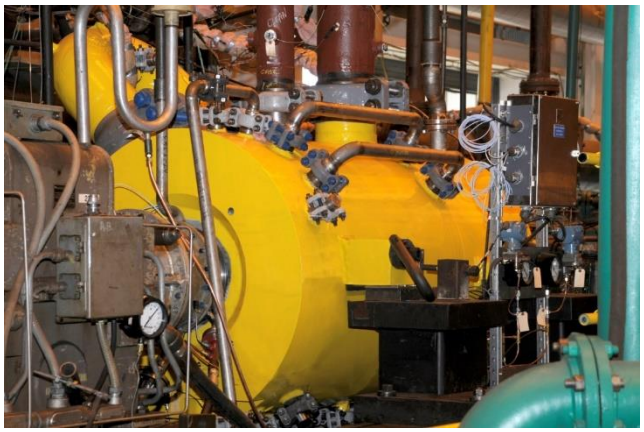

Photo Courtesy of Dresser-Rand, A Siemens Business

Figure 2: Tupi III Reinjection Compressor on Factory Test Stand

Although these two projects likely represent the highest pressure and density applications to date for centrifugal compressors, potential applications continue to be planned and developed that may extend beyond these current existing limits. These extreme, demanding conditions, extending well into the dense phase region where the fluid properties deviate beyond that of an ideal gas require accurate predictions of thermophysical properties. Existing equations of state allow predictions into the dense phase regions encountered, but the accuracy of the prediction of these properties is often assumed or unknown. Confirmation of the accuracy of these property predictions is best demonstrated through the use of empirically based PVT (pressure-volume-temperature) data.

CALCULATION OF COMPRESSOR PERFORMANCE

Aside from the obvious measured parameters of pressure, temperature and flow rate, along with their associated ratios, a limited number of additional calculated parameters have been developed to describe compressor performance and allow more useful comparisons of performance among machines of varying process parameters and gas compositions. These are derived from the First Law of Thermodynamics and are widely used. They also form the basis of ASME PTC 10 (1997) and allow the comparison between predicted and actual compressor performance.

The first of these additional parameters is the head, or usable work, applied to the gas being compressed. In the equation below, the expression for head is provided using the polytropic thermodynamic model of the compression process. Other models (e.g. isentropic and isothermal) exist, but the polytropic model is most universally used for process compression applications. An examination of the equation for polytropic head shows that the measured parameters of pressure, temperature and gas molecular weight are required in the calculation. Additional parameters, such as gas specific volumes, gas compressibility, and polytropic exponent must be derived from some relation for thermophysical properties estimation. Derivation of these additional parameters for an ideal gas is relatively straightforward, however, determination of these parameters for real gas conditions represents more of a challenge. Two equal forms of the polytropic head equation are provided below and may be used interchangeably. Appendix A provides a more complete derivation of the polytropic head equation currently included in ASME PTC 10 (1997) and also provides further information on the isentropic head thermodynamic model.

$$Wp = C1 * f_s * \frac{n}{n-1} * [P_d * v_d - P_s * v_s] = C2 * f_s * \frac{Z_s * T_s}{MW} * \frac{n}{n-1} * \left[\left(\frac{P_d}{P_s}\right)^{n-1/n} - 1\right] \quad \text{Eqn. 1}$$

$$where: n = ln\left(\frac{P_d}{P_s}\right)/ln\left(\frac{v_s}{v_d}\right)$$

The value of the polytropic head derived from Equation 1 above represents the usable portion of work (or energy) applied to the gas during the compression process to raise the pressure from suction to discharge conditions. This is only a portion of the total work required by the compressor. The additional work required is lost work and largely represented by a rise in the gas temperature. Equation 2 below represents the ratio between the polytropic head and total work required in the compression process and provides the value of polytropic efficiency for the compression process. In addition to the thermophysical properties identified in the equation for polytropic head above, values for the additional property of enthalpy at suction and discharge conditions is required. Similarly, values for enthalpy under ideal gas conditions are relatively easy to derive, but become more difficult for real gases.

$$\eta_p = Wp/(C3 * (h_d - h_s)) \quad \text{Eqn. 2}$$

A final fundamental parameter necessary for the description of compressor performance is the absorbed gas power. This is provided in the following Equation 3 and is simply a combination of the measured mass flow rate and the two parameters defined above. Accurate estimation of the required horsepower for a compression process also requires accurate thermophysical parameter estimation.

$$PWR = C4 * \dot{m} * Wp/\eta_p = C5 * \dot{m} * (h_d - h_s) \quad \text{Eqn. 3}$$

These additional thermophysical properties can be obtained from an equation of state for any specific gas or gas mixture. Of course, the simplest of these would be the ideal gas equation with the compressibility factor equaling unity and the gas specific volume calculated using the values of pressure, temperature and gas molecular weight. In the case of a real gas, the compressibility factor will need to be derived from any one of a number of equations of state in existence. Many of these different equations of state are expressed in terms where the compressibility factor is either derived explicitly or, more commonly, through some iterative procedure. The compressibility factor may then either be used directly in Equation 1 or to determine the real gas specific volume, v_{real}, at suction and discharge conditions. It should be noted that the Schultz correction factor, f_S, requires additional properties of enthalpy and entropy to be derived, but the value of this variable generally tends to be very close to unity and may be neglected for an initial estimate of the polytropic head. Sandberg and Colby (2013) have also shown that at extreme conditions the Schultz factor may actually predict an unacceptable correction and should be replaced with an alternative method.

$$Z = (P * MW * v_{real})/(R * T) = v_{real}/v_{ideal} = \rho_{ideal}/\rho_{real} \quad \text{Eqn. 4}$$

The remaining necessary properties, enthalpy and entropy, are expressed as the combination of the value of these parameters at ideal conditions and some departure from ideal. Enthalpy of an ideal gas can be calculated by integrating the constant pressure specific heat across some temperature differential. The value of the constant pressure specific heat is normally also a function of the temperature which makes the integration more complex but nevertheless solvable. Since the real gas enthalpy is considered to be a function of both pressure and temperature, this results in the departure enthalpy becoming a function of the pressure. Equation 5 provides the basis of calculating the real gas enthalpy (or enthalpy differential) for any gas.

$$\Delta h_{real} = \Delta h_{ideal} + \Delta h_{departure} \quad \text{Eqn.5}$$

A similar relation exists for the determination of the real gas entropy, again being the summation of the value at ideal conditions and some departure from ideal. This is provided in Equation 6 below. The ideal entropy is similar to ideal enthalpy in that it is an expression which is an integral over some temperature range. In the case of ideal entropy, the value of the function integrated is the constant pressure specific heat divided by the temperature summed with a function of the pressure related to a reference pressure. It should be noted that the expressions for both enthalpy and entropy are expressed as differentials. These differentials can be assumed to be calculated as differences between suction and discharge conditions, however, they can also be related to some common reference condition to provide point values of these parameters. It is also possible to express these equations in terms of total enthalpy and entropy instead of specific values as shown herein.

$$\Delta s_{real} = \Delta s_{ideal} + \Delta s_{departure} \quad \text{Eqn.6}$$

Values of real gas enthalpy and entropy require further explanation as to the method of deriving the departure values of these parameters. Equation 7 provides the relationship for calculating departure enthalpy. Inspection of this equation shows that the departure value is related to the gas measured values of pressure, temperature, molecular weight and the compressibility factor integrated over some pressure interval. Although this is a complex relationship, more simplified, integrated expressions have been derived for a number of the different equations of state in existence for this parameter.

$$\Delta h_{departure} = -\int \frac{R*T^2}{P*MW}\left(\frac{\partial Z}{\partial T}\right)_P dP \quad \text{Eqn. 7}$$

The equivalent relationship for the departure values of entropy is provided in Equation 8. It is also shown to be a function of the measured parameters of pressure, temperature, gas molecular weight and compressibility factor. This complex relation has also been further derived for many of the different real gas equations of state in existence. Appendix B provides a more detailed derivation of these departure functions along with relations for the ideal gas properties.

$$\Delta s_{departure} = -\int [\frac{Z*R}{P*MW} + \frac{R*T}{P*MW}\left(\frac{\partial Z}{\partial T}\right)_P]dP \quad \text{Eqn. 8}$$

An important point to note is that the compressibility factor and its relationship to pressure and temperature allow prediction of the departure functions for enthalpy and entropy. While this is not a consideration normally given due to the fact that many of the equations of state for real gases in existence already have these parameters expressed in a more easily calculable form, it should be noted that if an empirically based relationship between the compressibility factor and pressure and temperature exists, an alternative method to calculate these functional values can be derived.

EQUATIONS OF STATE AND PVT DATA

Equations of State

As noted above, several different equations of state have been developed to describe real fluid behavior. Some of these have been very focused and limited in their application to different gases, but others have been developed to be utilized for a wide range of individual components and mixtures at the potential expense of reduced accuracy. Most of the currently used equations of state have evolved from two basic relations, the van der Waals and the Beattie-Bridgeman equations of state. The cubic equations of state have developed from the original van der Waals equation, whereas the virial forms have been transformed from the Beattie-Bridgeman equation. A third fundamental equation of state class has been originated in recent years based upon mixed fluid properties and has the Helmholtz energy explicitly related to the fluid density and temperature.

Six different equations of state have been included in this study. They were selected based upon their current usage in gas compression applications, process simulation evaluations, and potential enhanced capability of other equations of state. The thermophysical properties evaluated by these six different equations of state will include the compressibility factor, departure enthalpy, and departure entropy.

Three of the six equations can be classified as cubic equations of state. The first of these, the Redlich-Kwong, R-K, (1949) equation of state is one of the more basic forms of the cubic equation of state family and has served as the basis of further developments. While the Soave modification, SRK, of the Redlich-Kwong equation of state is an advancement, it is considered to be incremental to the Peng-Robinson, P-R, (1976) equation which will be included. The SRK and P-R equations of state involve relationships including a third parameter, the acentric factor, to improve property predictions. The acentric factor is a parameter that relates to molecular geometry and polarity. A final cubic equation of state form, the volume translated Peng-Robinson, VTPR, as defined by Jhaveri and Youngren (1988), has been included to demonstrate the improvement in predictions over the R-K and P-R equations of state. Essentially the action of the volume translation parameter shifts the predicted specific volume (or compressibility factor) in order to improve its accuracy against actual PVT data. A number of volume translation methods have been proposed in the literature for the cubic equations of state family, however, the VTPR equation was selected due to its ease of application. Care should be exercised if alternative volume translation

methods are used to ensure comparable or improved accuracy of predictions. The cubic equations of state have remained popular although their accuracy has been demonstrated to be less than that of other relations, particularly at higher pressures. They continue to be utilized as the default equations of state in many commercially available process simulation software applications due to the fact that the volume (or compressibility) can be solved explicitly without the need for iteration. A solution for the compressibility factor with the equation of state is therefore assured without significant effort.

Two equations of state included in the evaluation can be considered variations of the virial equation of state. Virial equations of state utilize empirically based constants, whereas the cubic equations of state are primarily only dependent upon physical constants of the components involved. The first of these, the Benedict-Webb-Rubin-Starling (BWRS) equation as modified by Lin and Hopke (1974), has been used extensively in compressor performance calculations due to its perceived accuracy, particularly associated with hydrocarbon mixtures. A second equation, the Lee-Kesler-Plocker, LKP, (1978) equation of state, is a generalized form of the original Benedict-Webb-Rubin equation of state utilizing a comparison of the gas mixture against two reference fluids (one with a small and one with a large value of the acentric factor) that provide constants for the equation. The LKP equation of state has been recognized as a very accurate equation of state for use in a number of gas compression applications. Its evolution comes from the Principle of Corresponding States which is an observation that all gases behave in a comparable manner when dimensionless independent parameters are utilized.

The sixth and final equation of state to be evaluated is the GERG-2008, GERG, Kunz and Wagner (2012), equation as implemented in the NIST REFPROP, Lemmon, et al. (2010), software application. Although relatively new, the GERG equation of state has been widely lauded as providing superior accuracy in the prediction of properties for a number of gases and gas mixtures, including commercial and industrial refrigerants. The 2008 implementation of this equation and its associated property derivatives includes a large number of empirically based constants based upon 21 gas components that are relatively common in industry. It continues to receive growing recognition as a plausible equation of state to be used for gas compression performance evaluations.

PVT Data

Experimentally based pressure-volume-temperature (PVT) data is critical in not only calibrating constants in a number of the different equations of state, but also serves as a source of validation of the accuracy of any equation of state or to identify prediction differences between equations of state. This data is typically collected in one of two formats, namely along isotherms or isochores. In the case of isothermal data, the dependent variable of specific volume (or compressibility factor) is measured at a constant temperature over a variable range of pressure. Isochoric, or constant specific volume, data is obtained by maintaining a constant sample density with variations in temperature and pressure. The most prevalent type of PVT data currently available is isothermal in nature and has been used in this study. Although the compressibility factor is obtained at discrete temperatures over a range of pressure, this data represents a continuous three-dimensional surface with the independent variables of pressure and temperature establishing the dependent value of compressibility factor. This is illustrated in Figure 3 below, which has been generated from actual PVT data for a 90% methane/10% propane mixture.

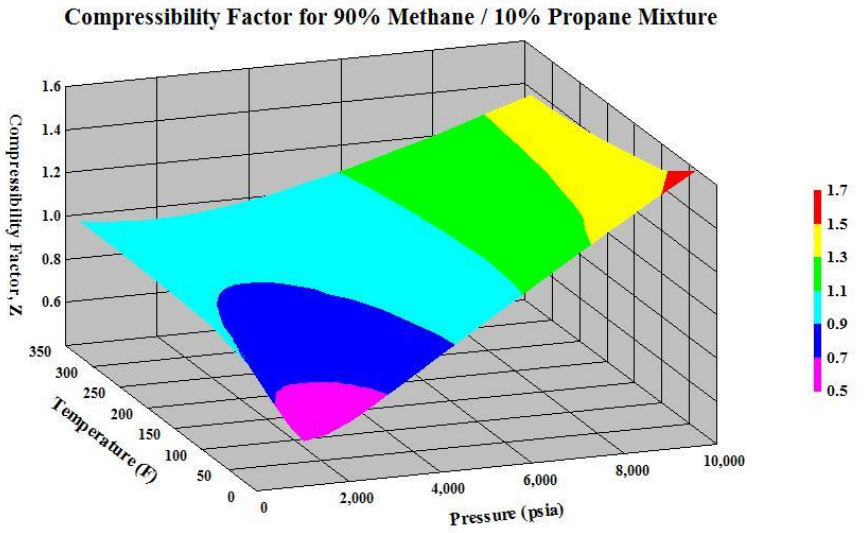

Figure 3: Compressibility Factor Surface

An examination of Figure 3 shows that the compressibility factor steeply declines when the pressure is raised continually to approximately 2000 psia after which it nearly linearly increases thereafter at lower temperature levels. Conversely, at the higher temperature parts of the range, the behavior of the gas mixture rises more gradually from a compressibility factor of nearly unity at lower pressures to levels near that of the maximum values noted at the lower temperatures. Such a variation in compressibility factor across the ranges of pressure and temperature demonstrate that a number of data sets need to be obtained to give a more accurate indication of the variability in the compressibility factor. More specifically, in the case of isothermal PVT data measurements, a temperature range extending beyond the expected compression range of temperatures with a minimum of four isotherms should be considered. Although different gases or mixtures of gases may behave differently, an approximation of the variation in compressibility factor across the range of anticipated pressures and temperatures should be completed. This can be obtained through either a set of calculations utilizing an equation of state or through an evaluation of a generalized compressibility factor data using gas critical pressure and temperature or gas mixture pseudo-critical pressure and temperature as prescribed in the Principle of Corresponding States.

Cubic Splines

While experimentally obtained PVT data is valuable in the comparison between measured and equation of state predicted values of specific volume or compressibility factor, the discrete nature of this data is not amenable to the calculation of the values of departure enthalpy and entropy at various pressures and temperatures. The relationships evident in Equations 7 and 8 show that to obtain the values of these parameters continuous functions of the compressibility factor are necessary to calculate the derivative and integral functions involved. A relatively accurate approximation of the continuous variation in the compressibility factor between experimentally derived points can be provided through the application of cubic spline interpolations. Cubic splines are piecewise continuous functions defined between discrete data points that are third-degree polynomial equations. This results in four constants that must be determined for each segment between data points. In order for the individual functions between data points to be continuous, the following constraints must be achieved:

1. The initial value of the function in any interval must be equal to the value of the data point and equal to the final value of the function in the previous interval.
2. The first derivative, or slope, of adjacent functions must be equal at the common data point.
3. The second derivative, or direction of curvature, of adjacent functions must be of the same sign at the common data point.

4. The final value of the function in any interval must be equal to the value of the data point and equal to the initial value of the function in the following interval.

These four constraints are sufficient to fully defined the constants associated with each internal piecewise continuous interval with the exception of the initial and final data points. Some assumption, such as equal slope, must be made for these initial and final data points. Accordingly, extrapolation of values beyond these points and any functional evaluation (e.g. derivatives) at or beyond the value at these end points is subject to error and should be avoided if possible.

The solution method for the derived values of departure enthalpy and entropy may then be summarized as follows:

1. Formulate cubic spline interpolation functions for the compressibility factor versus pressure for each isotherm of experimental PVT data.
2. Determine the value of compressibility factor at discrete values of pressure for each isotherm. Each of these predicted data sets will then be used for formulate additional cubic spline interpolations of compressibility factor versus temperature at each discrete pressure.
3. Numerically determine the differential of compressibility factor relative to temperature along an isotherm for each discrete value of pressure. These data points may then be used to establish an additional cubic spline interpolation of the derivative of compressibility factor relative to temperature along a range of pressures.
4. The cubic spline interpolations for compressibility factor versus pressure and derivative of the compressibility factor versus temperature along an isotherm may then be numerically integrated according to Equations 7 and 8 to derive values of the departure enthalpy and entropy based upon the experimental PVT data.

The experimentally derived values of departure enthalpy and entropy may then be compared against predictions of these parameters from various equations of state to assess the potential accuracy of any given equation of state to predict these values. It should be noted that the total values of the enthalpy and entropy require that the departure values be combined with the ideal gas values which are solely a function of the temperature. Additionally, the differences between these parameters from suction to discharge conditions in a compression process are only valid due to the fact that point values of these parameters at suction and discharge will also be related to some reference condition which may be different among the various equations of state. Therefore, any evaluations of relative accuracy in the prediction of values for the total enthalpy and entropy will be influenced by these modifications.

ANALYSIS OF ACTUAL PVT DATA

Eleven separate PVT data sets were evaluated against the six identified equations of state. These data sets were selected based upon their availability in the technical literature, variability in composition and chemical properties, and potential inclusion in industrially significant processes. Both single component and mixture data sets were included in an effort to demonstrate the relative accuracies of the various equations of state. Although a few of the data sets provided both isochoric and isothermal data, the majority of the data was only available as isotherms. The isothermal data format was only analyzed in this evaluation.

Compressibility factors were calculated for each of the data points and compared against the values predicted from each equation of state. Additionally, cubic splines were fitted to the data and numerical derivatives and integrals were evaluated as previously defined utilizing the MathCAD software application to estimate experimentally derived values of departure enthalpy and entropy for each of the PVT data points. These were also compared to equation of state based estimates of these parameters.

Multiple isotherms were included for each separate gas composition PVT data set. Each isotherm was evaluated for the deviations in compressibility factor, departure enthalpy, and departure entropy, however, only a single set of figures of these parameters will be presented for each different gas composition. The presented information will be for a single isotherm at or near the middle of the involved temperature range. This is being done to minimize the amount of figures included in the paper and also to concentrate on the results from the middle of the temperature range where the results of the numerical integrations are presumed to be most accurate. It should be reiterated that the numerical approximations completed at the extents of the temperature range are most subject to errors. Error analysis is provided for deviations between the experimental values of compressibility factor and those provided by each equation of state. Although a similar analysis of deviations could be provided for the departure enthalpy and entropy, it has been previously

mentioned that this is of questionable value since these parameters must be added to their relative ideal gas values to arrive at the total point values of these parameters. Since the relative magnitudes of ideal gas and departure properties vary according to their reduced temperature values, any comparison is subject to considerable error.

The statistical analysis of deviations between the compressibility factor derived from a specific equation of state and the experimentally established value will be provided for all data points and all isotherms included in the data set for each gas composition evaluated. Three statistical parameters will be provided that represent the accuracy of each equation of state examined. These are:

1. Bias - The bias is defined as being the simple arithmetic mean of the deviations between the experimental PVT value of the compressibility factor and that predicted by a specific equation of state for all data points in the data set for each gas composition.
2. Average Absolute Deviation (AAD) - The AAD is the mean value of the sum of absolute values of deviations between the experimental PVT value of the compressibility factor and that predicted by a specific equation of state for all data points in the data set for each gas composition. It should be noted that if the magnitude of the bias and AAD are equal, this reflects that the particular equation of state consistently over or under predicts the compressibility factor depending upon the sign (positive or negative) of the bias.
3. Root Mean Squared Deviation (RMS) - The RMS deviation is a measure of the relative scatter of deviations between all of the points in the data set. It is the standard deviation of the data set, with a value closer to the magnitude of the AAD representing a more consistent deviation between predicted and experimental value across the range of data points.

Methane

The first single component gas to be evaluated is methane. PVT data for pure methane was obtained from the relatively recent publication by Cristancho, et al. (2010). Methane is a desirable gas with which to begin due to its relatively simple and uniform molecular structure. This is reflected through the value of its acentric factor of 0.0108 which is relatively low in comparison to the other gases examined. A small value of the acentric factor corresponds to a more spherically shaped molecule with a small amount of polarity. Accordingly, more accurate prediction of properties should be provided through an equation of state. The PVT data set is composed of five different isotherms with temperatures ranging from 77 F to 350 F (25 C to 176.7 C). This corresponds to reduced temperatures, Tr, ranging from 1.56 to 2.36 and reduced pressures, Pr, reaching values greater than 30. Figure 4 provides a comparison of predicted and measured compressibility factors for a temperature of 149 F (65 C).

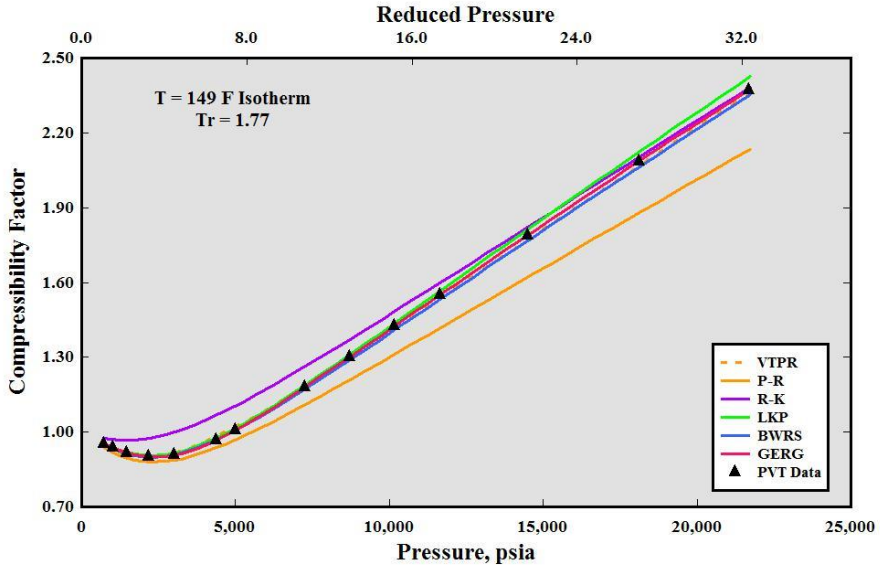

Figure 4: Compressibility Factor for Methane

It is evident from the graph above that all but the R-K and P-R equations of state compare favorably with their predictions of compressibility factor across the range of pressures reaching more than 20,000 psia (1379 bara). The R-K equation of state over predicts compressibility factor at lower pressures within the range, whereas the PR equation of state under predicts compressibility factor at pressures above 5000 psia (345 bara).

A comparison of predicted and derived values of the departure enthalpy are provided in Figure 5 for the same isotherm of 149 F (65 C).

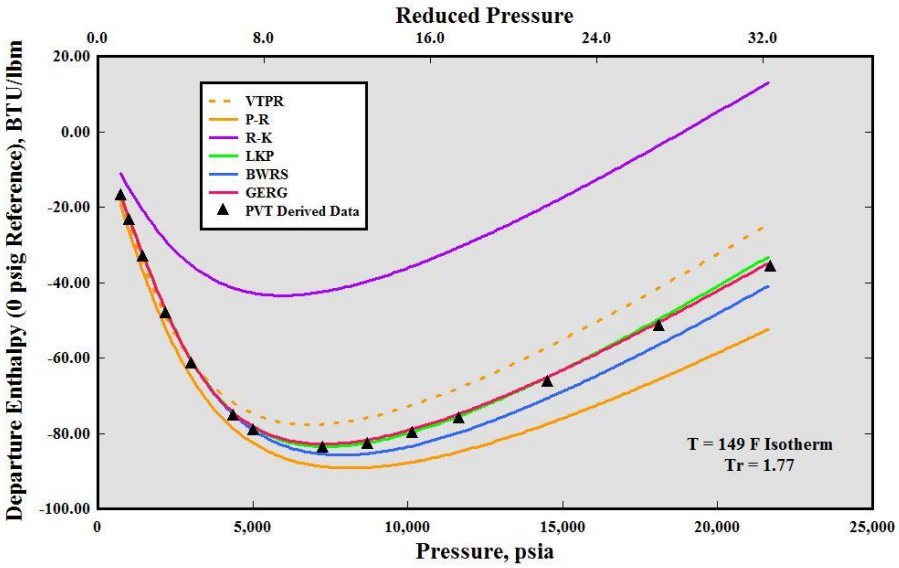

Figure 5: Departure Enthalpy for Methane

With the exception of the R-K equation of state, predictions of departure enthalpy for the remaining five equations of state at this temperature level appear to be fairly consistent. At elevated pressures, the GERG and LKP equation of state appear to correlate more closely to the experimentally derived values. These results are relatively the same across the entire temperature range evaluated. Accuracy for methane departure enthalpy at this range of reduced temperatures is relatively insensitive due to the magnitude of the departure value to the total value of up to approximately 20%. This relative amount diminishes at the higher end of the temperature range.

Figure 6 provides a comparison of the predicted and derived values of departure entropy for the same temperature.

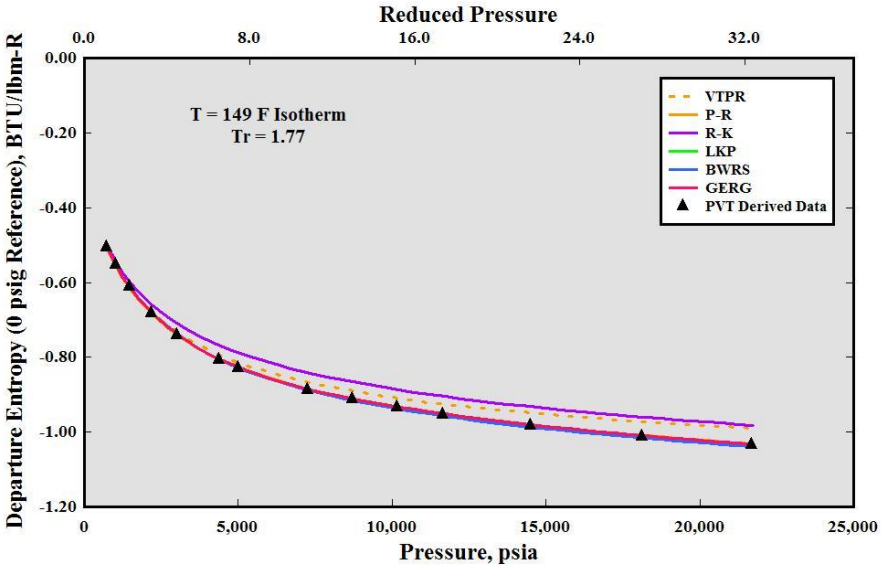

Figure 6: Departure Entropy for Methane

Here the predicted values for all equations of state with the exception of R-K and VTPR agree very well with the experimentally derived values of departure entropy. These results confirm that a number of the different equations of state provide accurate predictions of methane properties across a wide range of pressures and temperatures, particularly at increasingly higher values of pressure.

A statistical analysis of the percentage deviations between the experimentally based values of the compressibility factor and the predictions from the six evaluated equations of state is presented in Figure 7 below. This is based upon results from 74 data points distributed over five isotherms.

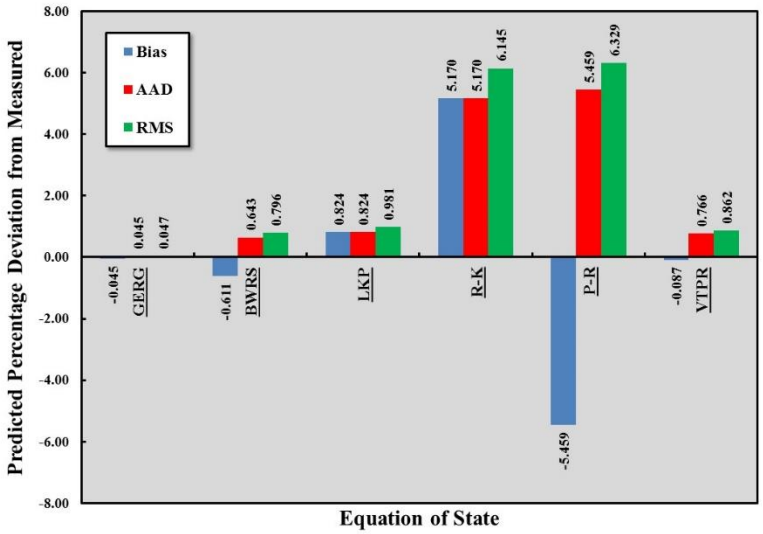

Figure 7: Compressibility Factor Percentage Deviations for Methane

Clearly the GERG equation of state provides superior predictions of the thermodynamic properties of interest. The BWRS and LKP equations of state also offer reasonable predictions, with the BWRS equation of state being more accurate for compressibility factor

while the LKP equation of state appears to offer a more accurate prediction of enthalpy. The VTPR equation of state may offer reasonable estimates, but the values for the departure enthalpy and entropy appear to deviate more than BWRS. The R-K and P-R equations of state failed to provide reasonable accuracy, particularly at elevated pressures.

Nitrogen

The next single component gas to be examined is the diatomic molecule, nitrogen. Due to its relative abundance and favorable properties, it is widely used in industry for such applications as tank blanketing and inerting, cryogenic refrigeration, and high pressure injection for enhanced recovery of reservoir fluids. It is also commonly used as a gas component in factory acceptance testing of compressors. PVT data for nitrogen was obtained from the relatively recent publication by Mantilla, et al. (2010) and the same research group from Texas A&M University that completed the work on methane. Although the acentric factor for nitrogen is higher than methane with a value of 0.0370, it is still much lower than that of carbon dioxide or water.

The PVT data set for nitrogen is also composed of five different isotherms with temperatures ranging from 17 F to 260 F (-8.3 C to 126.7 C). This corresponds to higher reduced temperatures, Tr, ranging from 2.10 to 3.17 with reduced pressures, Pr, reaching values greater than 40. Figure 8 presents a comparison of predicted and measured compressibility factors for a temperature of 170 F (76.7 C).

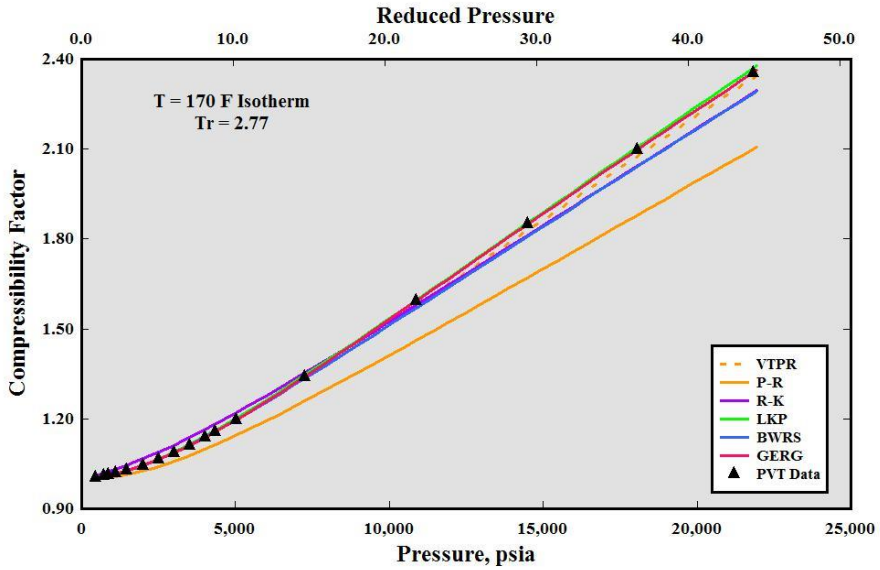

Figure 8: Compressibility Factor for Nitrogen

It is once again evident that the R-K and P-R equations of state show increased deviation from the experimental data compared to the other equations of state evaluated. The P-R equation of state, in particular, demonstrates increasing deviation at progressively higher pressures.

A comparison of departure enthalpy for nitrogen at 170 F (76.7 C) is provided below:

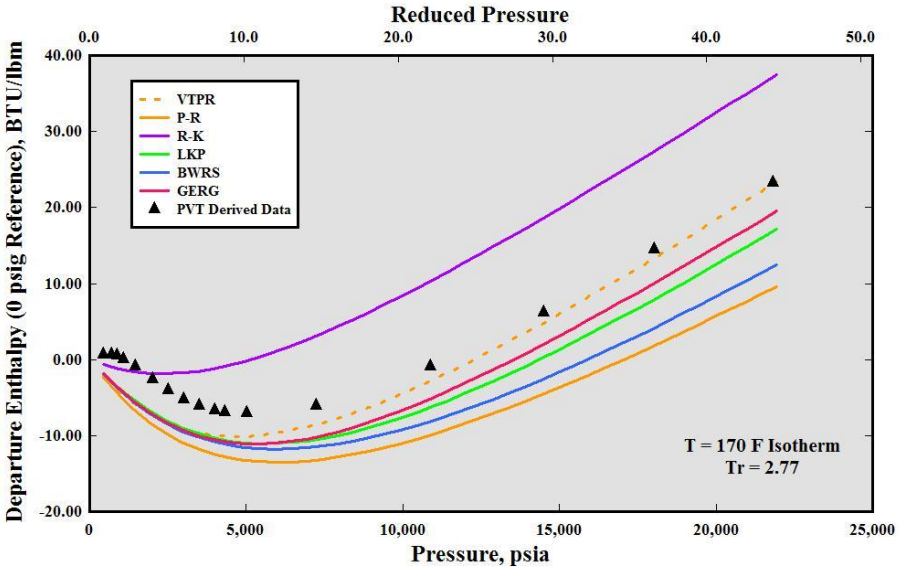

Figure 9: Departure Enthalpy for Nitrogen

The obvious level of more deviation between the experimentally derived values of departure enthalpy and those predicted by the various equations of state may initially result in some concern regarding the accuracy of these predictions, but the magnitude of the departure enthalpy should be compared against that of methane. It represents less than 10% of the total value of the sum of the ideal and departure enthalpies. Furthermore, given the relatively high values of reduced temperature, these isotherms are located well into the superheat region and at lower pressures do not exhibit significant curvature as pressures increase, resulting in minimal influence of pressure on the magnitude of the total enthalpy. Although it is believed that these deviations are relatively small and do not substantially impact the predicted values of total enthalpy, this nevertheless warrants some additional investigation.

Values of departure entropy are presented in Figure 10 below:

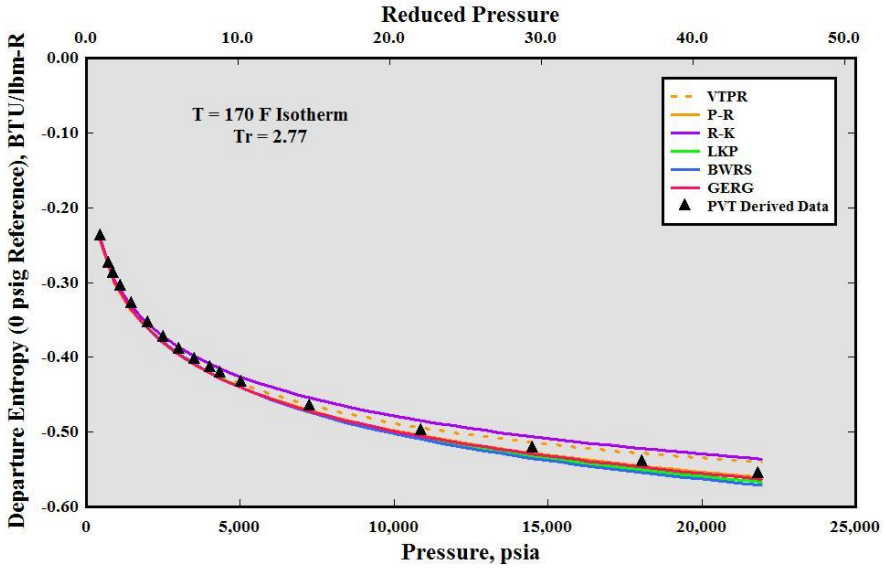

Figure 10: Departure Entropy for Nitrogen

Inspection of this plot demonstrates that there is good agreement between the derived experimental data and all equations of state with the exception of R-K and VTPR at higher pressure levels. Finally, looking at the deviation statistics for all five isotherms, representing 77 data points.

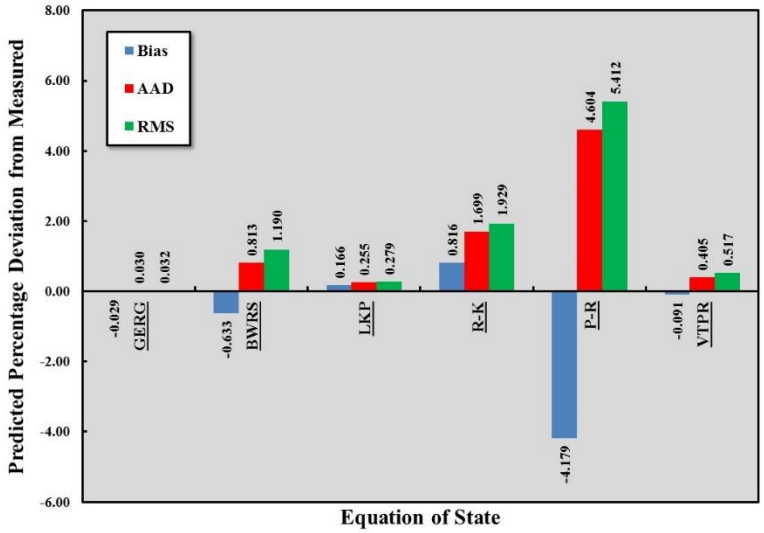

Figure 11: Compressibility Factor Percentage Deviations for Nitrogen

Similar to the results for methane, four of the six equations of state display their ability to accurately predict the compressibility factor and presumably the additional thermodynamic parameters. Both GERG and LKP reflect predictions of compressibility factor across the entire pressure and temperature range within 0.5%, followed by VTPR and BWRS having predictions within 1.5%. The R-K and P-R equations of state produce values beyond this and should be questioned in their accuracy, particularly at higher pressure levels.

Carbon Dioxide

The third and final single component gas to be examined is carbon dioxide. Like nitrogen and methane, carbon dioxide is commonly encountered in industrial processes, whether in a mixture or as a single component gas. Carbon dioxide is unique in many of its behaviors relative to most other gases and gas mixtures due to the proximity of its critical pressure and temperature to process conditions commonly found in industry. The experimental data set, also obtained by the same research group at Texas A&M University and authored by Mantilla et al. (2010), is composed of four isotherms with a temperature range from 90 F to 350 F (32 C to 176.7 C). This is equivalent to reduced temperatures from a minimum of 1.02 to a maximum value of 1.48 with reduced pressures extending to a value near 20. Carbon dioxide possesses an acentric factor of 0.2667 which is significantly higher than that of nitrogen and methane, suggesting a more non-uniform molecular structure. Experimentally measured compressibility factors at 260 F (126.7 C) and those predicted by the six equations of state are provided in Figure 12.

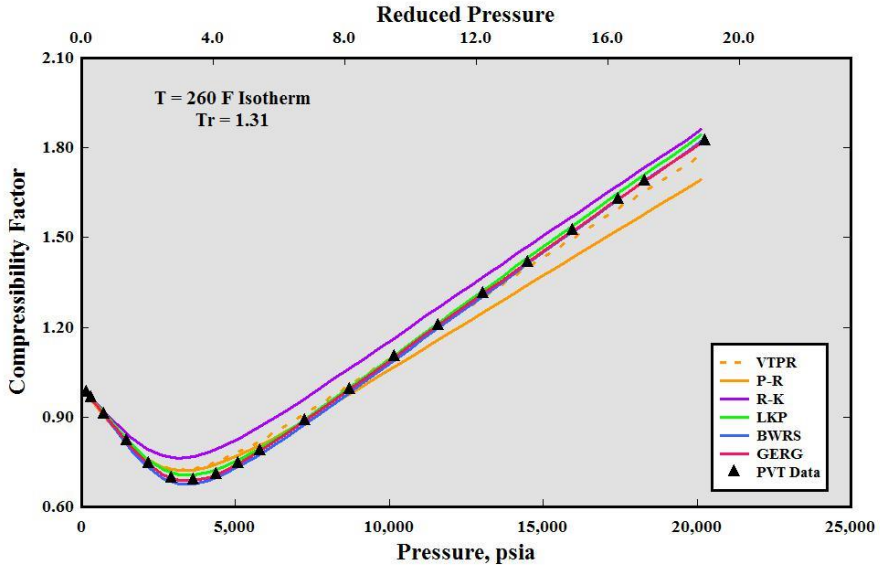

Figure 12: Compressibility Factor for Carbon Dioxide

Results for empirically measured compressibility factor versus equation of state predicted values are consistent with the previous two single component gases with respect to accuracy. GERG, LKP and BWRS equations of state appear to deliver closer predictions, whereas the R-K and P-R equations of state demonstrate more significant deviations. At the specific temperature of 260 F (126.7 C) provided above, GERG and BWRS show closer agreement near the compressibility factor minimum located in the 2500 psia to 4000 psia (172 to 276 bara) pressure range.

The departure enthalpy data for carbon dioxide is provided in Figure 13 below.

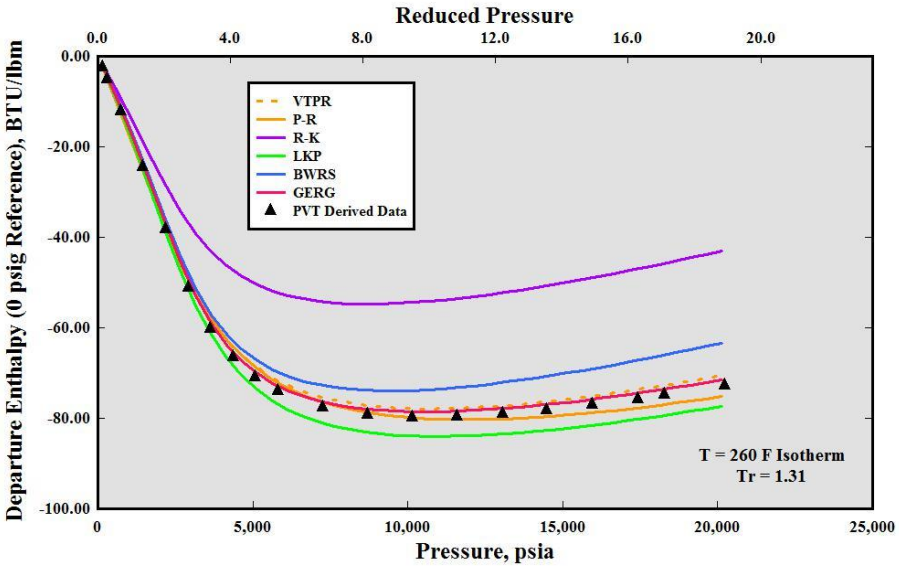

Figure 13: Departure Enthalpy for Carbon Dioxide

There is good agreement between equation of state predicted and experimentally derived values of departure enthalpy with the exception of the R-K equation of state at lower pressures within the range. At pressures exceeding approximately 5000 psia (345 bara), the GERG,

VTPR, and P-R equations of state show closer agreement with LKP and BWRS representing larger deviations. The percentage of departure enthalpy to total enthalpy for carbon dioxide within this temperature range approaches 50% with larger values at the lower temperatures of the range. Accuracy of calculations utilizing enthalpy may be impacted as pressures are raised to the upper part of the pressure range.

Results for the departure entropy are provided in the following plot and are similar in comparison to the other gases studied thus far in their agreement with the experimentally derived values.

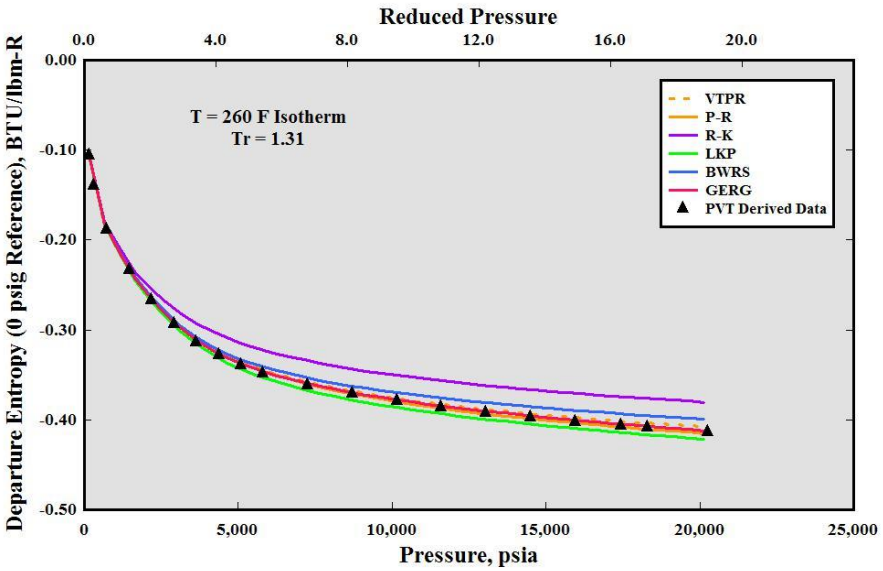

Figure 14: Departure Entropy for Carbon Dioxide

The ability of the different equations of state to accurately predict the compressibility factor for pure carbon dioxide across the range of temperatures evaluated is presented in Figure 15. These percentage deviations are based upon 49 measured points.

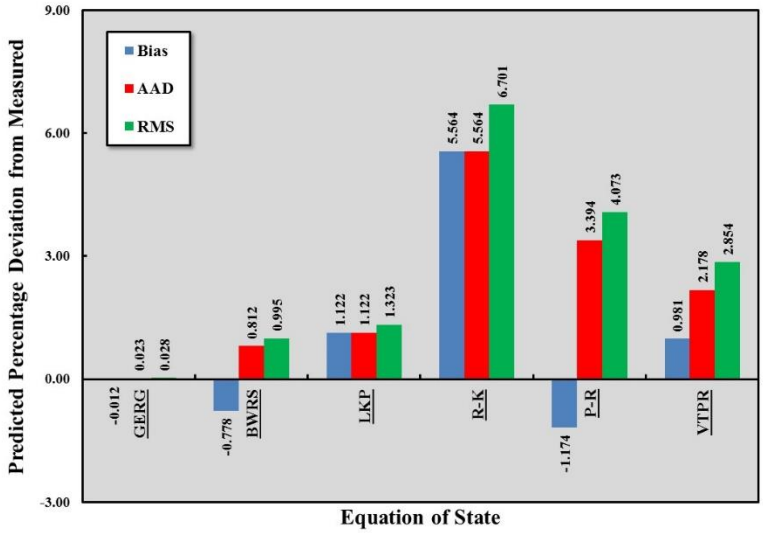

Figure 15: Compressibility Factor Percentage Deviations for Carbon Dioxide

Results are consistent with methane and nitrogen in that the GERG, LKP and BWRS equations of state show closer agreement with the experimental data. The majority of the deviations are within 1.5% of the test data with GERG representing superior predictability. The R-K, P-R and VTPR equations of state show increased inaccuracy with the R-K equation of state RMS value near 7% and continuous over-prediction of the compressibility factor.

Natural Gas

Although more prevalent in actual practice, gas mixtures have the potential to represent a more challenging case for equations of state to accurately predict thermophysical properties. This is primarily due to possible interactions between the different components of the gas mixture. Probably the most common gas mixture encountered in industry is natural gas. Natural gas is generally composed primarily of light paraffinic hydrocarbons, however, small amounts of other hydrocarbons and other components such as nitrogen, carbon dioxide, and hydrogen sulfide are commonly found.

Two different natural gas mixtures will be evaluated in this study. The first is classified as a sweet natural gas with only paraffinic hydrocarbons through pentane included in the mixture. Composition of this sweet natural gas (designated as SNG-4) is approximately 90% methane, 5% ethane, 2% propane, 2% butane (roughly equally split between normal butane and iso-butane), and 1% pentane (roughly equally split between normal pentane and iso-pentane). The second natural gas mixture (designated as SNG-1) has a composition of approximately 90% methane, 3% ethane, 1.6% propane, 1.6% butane (roughly equally split between normal butane and iso-butane), 0.3% pentane (roughly equally split between normal pentane and iso-pentane), 1.7% nitrogen, and 1.7% carbon dioxide. The experimental PVT data for these two gas mixtures is provided in the papers by Atilhan, et al. (2011 and 2011), Cristancho et al. (2011) and McLinden (2011). Unfortunately, the PVT data bases contain only three isotherms each, increasing the uncertainty of the derivatives and integrals numerically calculated. In an effort to reduce this increased uncertainty, two additional isotherms were constructed using the REFPROP program to estimate compressibility factors between the temperature extremes and midpoint.

Sweet Natural Gas

The temperature range of the SNG-4 data set ranged from -10 F to 350 F (-23 C to 176.7 C), which corresponds to a reduced temperature range from a minimum value of 1.20 a maximum of 2.17. Reduced pressures reached values over 30.0. Behavior of the compressibility factor is consistent with that observed on the other gases evaluated thus far, with the R-K equation of state over predicting the value of the compressibility factor, particularly at low pressures, and the P-R equation of state under predicting at higher pressure levels. The remaining four equations of state predicted the compressibility factor relatively accurately across the entire range state. This is evident in Figure 16.

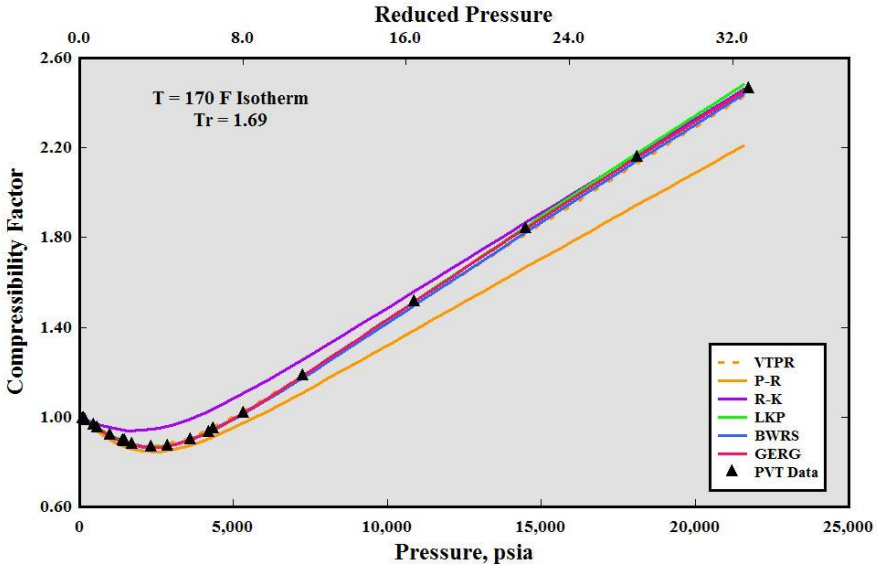

Figure 16: Compressibility Factor for Sweet Natural Gas

Derived values of departure enthalpy show increased deviation with most of the equation of state predictions. This is believed to be primarily influenced by the heavier hydrocarbons included in the mixture, even at their relatively low composition levels. The relative values of departure enthalpy to total enthalpy in this figure amount to approximately 15%. These characteristics are displayed in Figure 17.

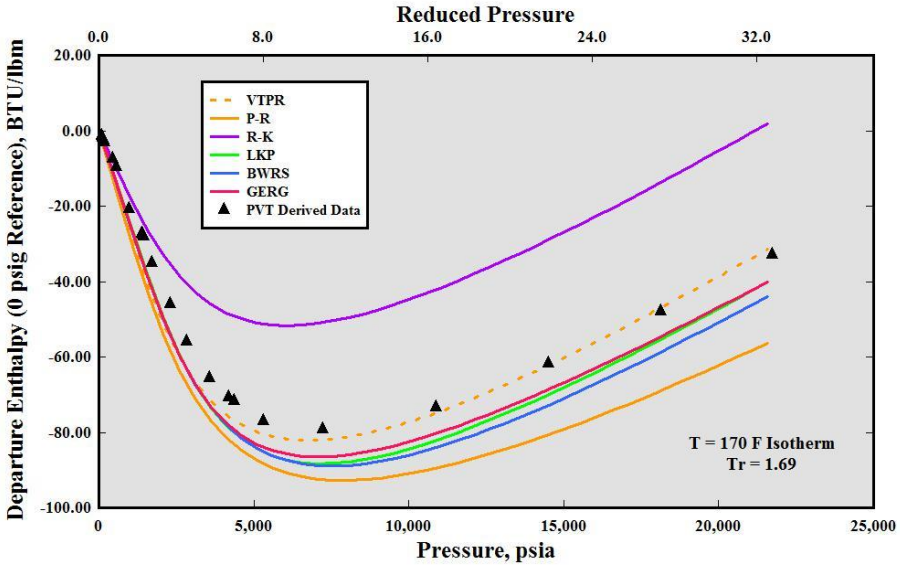

Figure 17: Departure Enthalpy for Sweet Natural Gas

Similar characteristics are demonstrated for the departure entropy as have been provided for the other gas samples. Most of the equations of state fairly accurately predict the departure entropy with the exception of the R-K equation of state at higher pressures. This is provided in Figure 18 below.

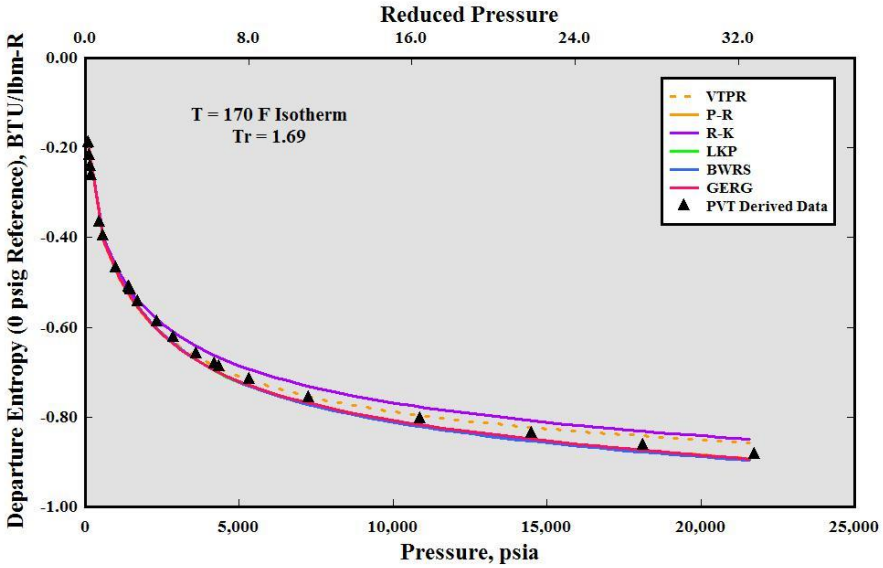

Figure 18: Departure Entropy for Sweet Natural Gas

The results of the statistical analysis of the compressibility factor deviations for all three isotherms is presented in Figure 19.

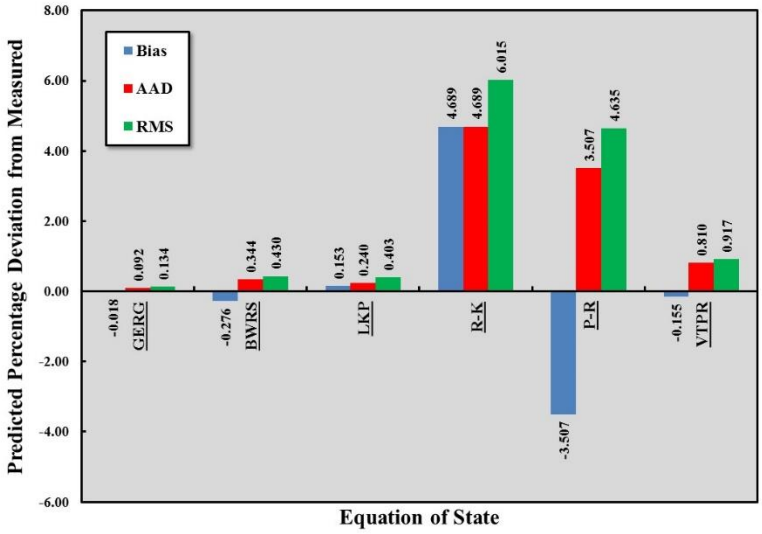

Figure 19: Compressibility Factor Percentage Deviations for Sweet Natural Gas

Typical Natural Gas

The second synthetic natural gas mixture (SNG-1) to be evaluated represents a more probable composition with small amounts of nitrogen and carbon dioxide present. As previously noted, the PVT data set contained only three isotherms which were supplemented by two additional isotherms developed with the REFPROP property software package. The reduced temperature range represented by this data varies from a minimum value of 1.23 to a maximum of approximately 2.23 with pressures ranging to a reduced pressure maximum of more than 30. A comparison of the experimentally determined compressibility factors and those predicted by the various equations of state is provided in Figure 20.

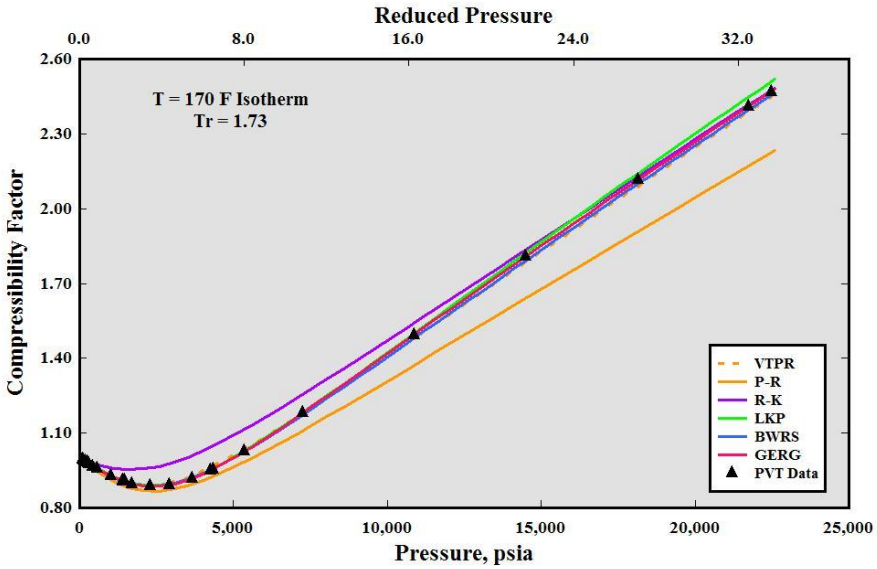

Figure 20: Compressibility Factor for Typical Natural Gas

Comparison of predicted and experimental values of the compressibility factor for this natural gas mixture are consistent with the sweet natural gas composition, with all but the R-K and P-R equations of state demonstrating close agreement across the entire range of pressure. Of course, the above figure covers only one isotherm, centered within the evaluated temperature range. It does provide insight into the behavior across the entire temperature range, though.

The departure enthalpy also displays similar characteristics across the pressure range as that of the sweet natural gas mixture. Individual equations of state show varying agreement with the experimentally derived values. In most cases, these differences are diminished due to the fact that the maximum portion of the departure enthalpy to total enthalpy is only approximately 15%. This is provided in Figure 21.

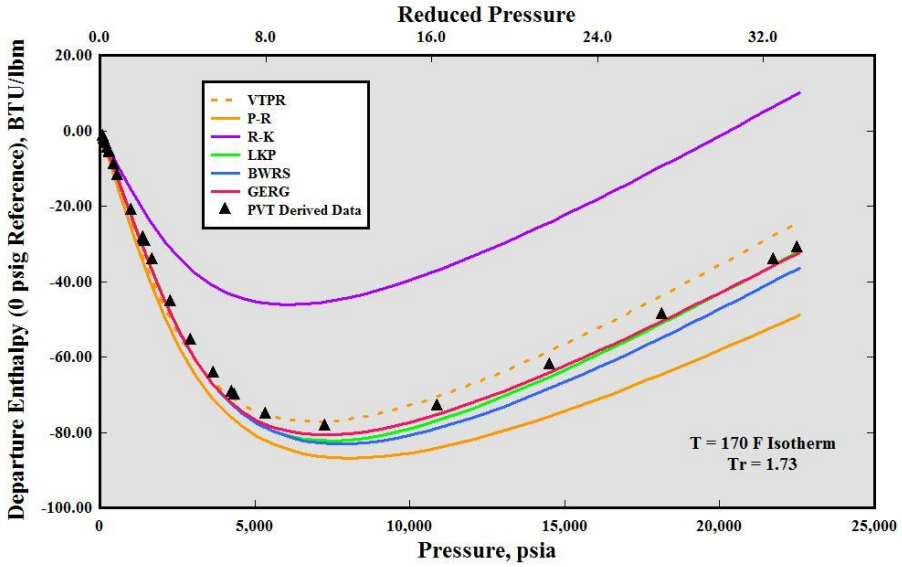

Figure 21: Departure Enthalpy for Typical Natural Gas

Departure entropy for the typical natural gas mixture is provided in Figure 22 and shows good agreement with all equations of state with the exception of R-K and VTPR at higher pressure levels. Consistent with the departure enthalpy, these differences are diminished with the ideal gas portion of the total entropy.

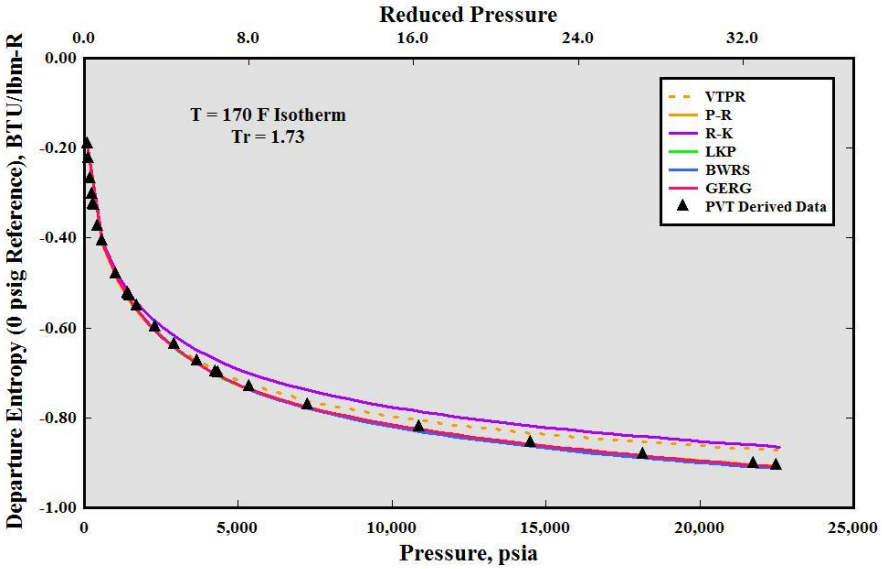

Figure 22: Departure Entropy for Typical Natural Gas

The compilation of compressibility factor statistics for all three isotherms is provided below in Figure 23. Results continue to demonstrate similar tendencies among the different equations of state. GERG, BWRS and LKP all show good agreement with the experimental PVT data. RMS values all fall below 1% with GERG reflecting superior performance. R-K and P-R equations show considerably higher deviations with P-R above 5%. R-K prediction errors are uniformly above empirical compressibility factors whereas P-R uniformly under-predicts the magnitude. This is evident from the relative values of Bias and AAD for these data sets.

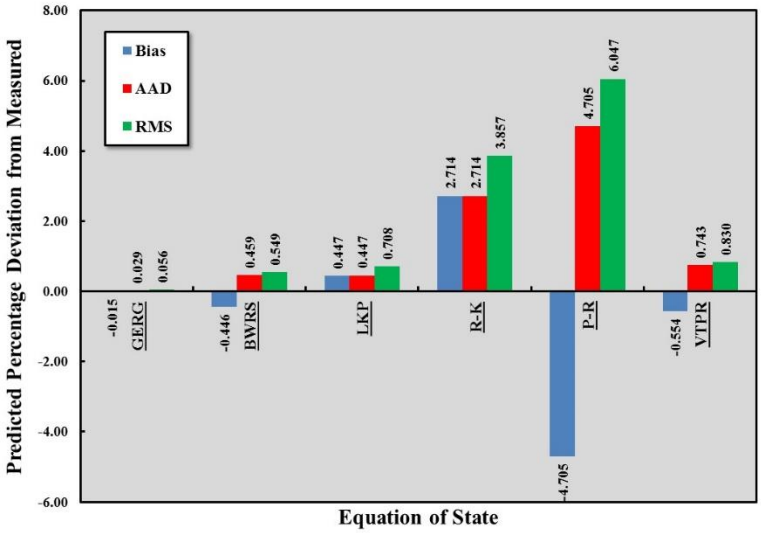

Figure 23: Compressibility Factor Percentage Deviations for Typical Natural Gas

Ethane – Carbon Dioxide Mixture

The next gas mixtures to be evaluated are composed of binary mixtures of ethane and carbon dioxide. Each mixture is composed of roughly 80% of one of the two components and 20% of the other. Variable compositions of gas mixtures including percentages of carbon dioxide in compression applications have experienced increasing frequency in enhanced oil recovery applications. Carbon dioxide rejection from gas sweetening processes mixed with associated natural gas to achieve flow rate requirements are reinjected to enhance the recovery of reservoir fluids. The carbon dioxide content can gradually change as some of the reinjected gas will once again be produced at the surface to be recycled back into the reservoir.

PVT data sourced for this evaluation is provided in the paper by Reamer, et al. (1945). Although dated, a significant amount of experimental data for a number of different gas mixtures from this group at the California Institute of Technology has been utilized and referenced in a number of other studies and publications over the years. Several papers containing PVT data from this group have been published in the technical literature.

83% Ethane – 17% Carbon Dioxide Mixture

The first of the two mixtures to be studied is composed of approximately 83% ethane and 17% carbon dioxide. Six isotherms were included in the PVT data set, ranging from 100 F to 400 F (37.8 C to 204 C) with pressures up to 10,000 psia (689 bara). This corresponds to a reduced temperature range of approximately 1.02 to 1.56 and reduced pressures reaching over 13.0. Information for the compressibility factor relationship is provided near the middle of the temperature range in Figure 24 below.

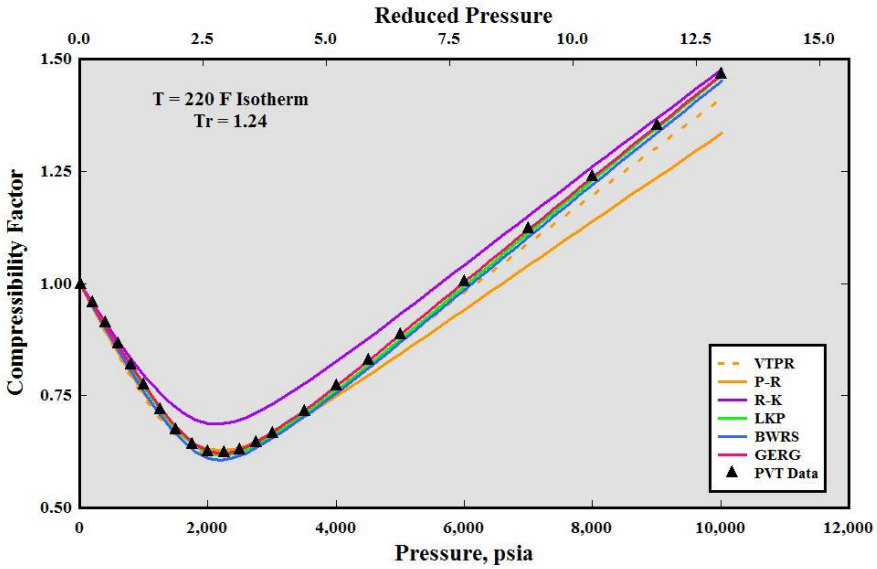

Figure 24: Compressibility Factor for Ethane / Carbon Dioxide Mixture

Close agreement between the empirical values and predictions appear to be relatively close for all equations of state below 1000 psia (69 bara). Deviations increase for the R-K equation of state above this pressure level with the predicted value consistently above that tested. The P-R equation of state continually under-predicts the value at pressures above 4000 psia (276 bara). The remaining equations of state provide reasonable predictions at all pressure levels across the range.

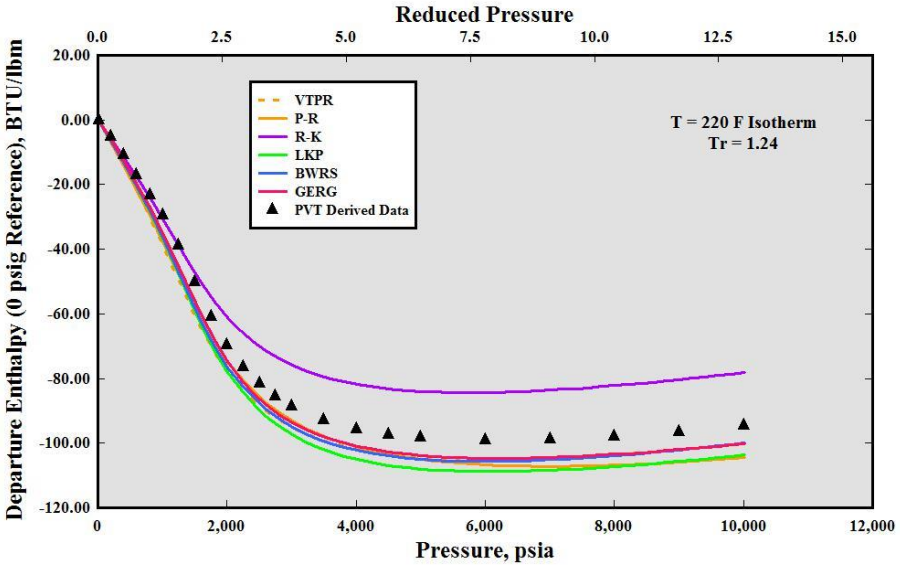

Figure 25: Departure Enthalpy for Ethane / Carbon Dioxide Mixture

Figure 25 presents a comparison of departure enthalpy between the derived experimental values and those predicted by the various equations of state. Relatively close agreement is noted among all equations of state except R-K, but the deviation between predicted and the derived values is increased at higher pressure levels. It should be noted that the isotherms directly adjacent to the one above show much closer agreement between tested and predicted values along the entire pressure range. The proportion of the departure enthalpy to total enthalpy value is roughly less than 30% at its maximum magnitude.

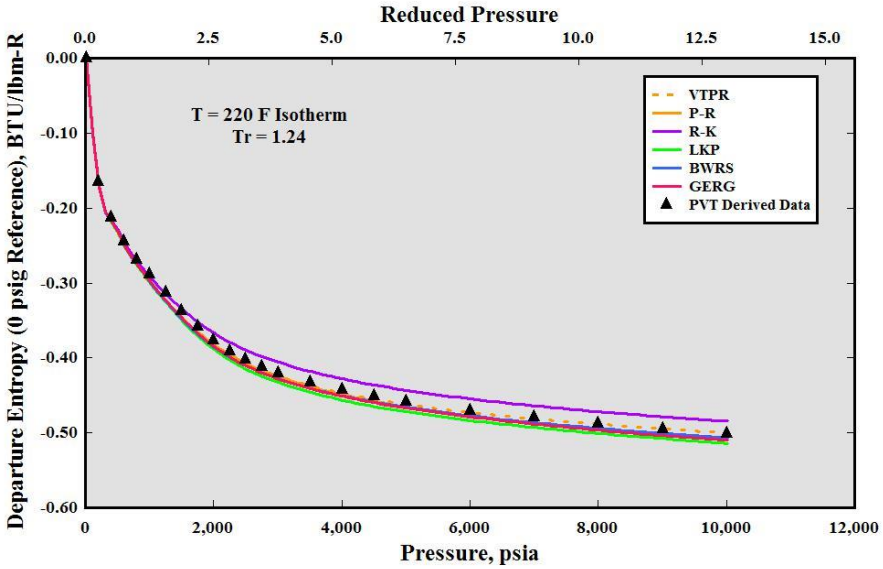

Figure 26: Departure Entropy for Ethane / Carbon Dioxide Mixture

Characteristics of the departure entropy are similar to all the other gases and gas mixtures presented thus far with relatively good agreement between the derived data and equation of state predicted values, possibly with the exception of R-K.

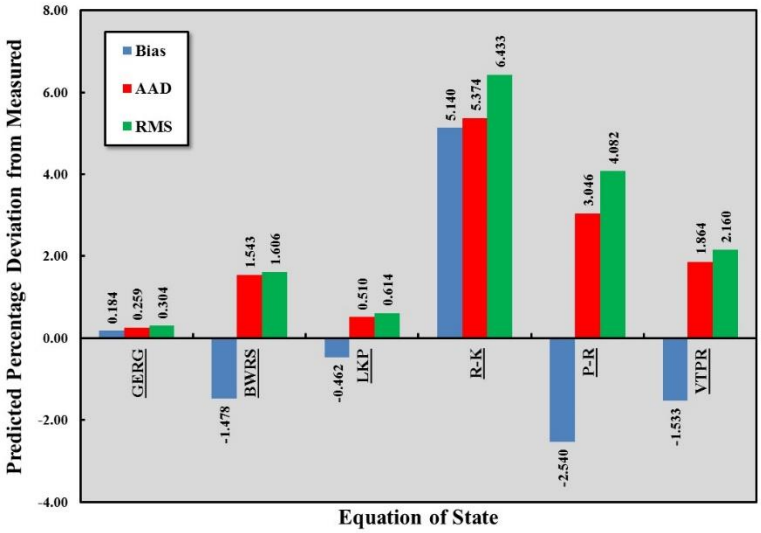

Figure 27: Compressibility Factor Percentage Deviations for Ethane / Carbon Dioxide Mixture

A compilation of the percentage deviations across all six isotherms is presented in Figure 27 above. GERG, BWRS and LKP equations of state result in RMS deviations less than 2%, whereas the others display greater average and RMS amplitudes.

18% Ethane – 82% Carbon Dioxide Mixture

The second hydrocarbon-carbon dioxide mixture to be examined is roughly a mirror image of the first, with carbon dioxide being the predominant component. In this case, the mole fraction of ethane is 17.77% and the amount of carbon dioxide is 82.23%. This results in only a slight difference in reduced properties with a reduced temperature range of 1.02 to 1.57 and a maximum reduced pressure of approximately 10.0. The compressibility factor plot is provided below as Figure 28.

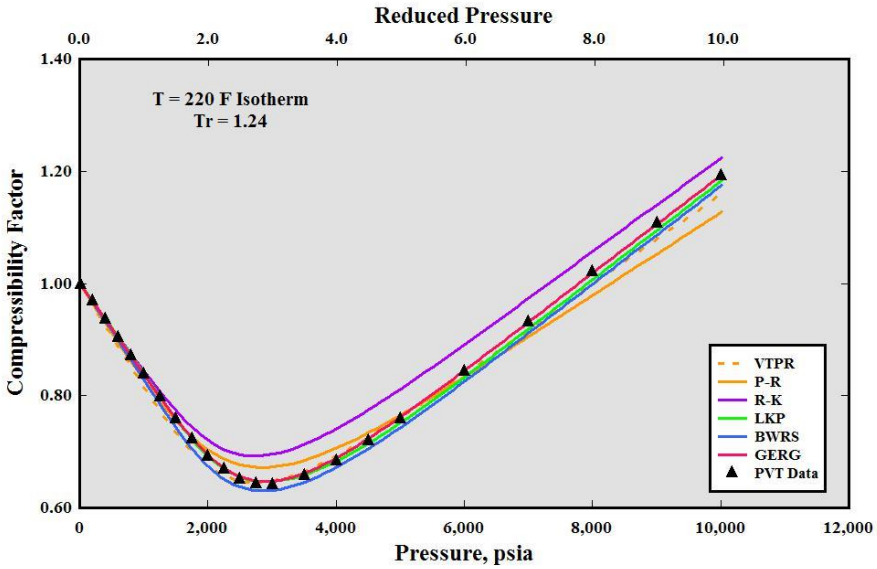

Figure 28: Compressibility Factor for Carbon Dioxide / Ethane Mixture

Departure enthalpy for this mixture is presented in Figure 29. In this case, agreement between the derived and predicted values is closest with the GERG, P-R and BWRS equations of state at the higher end of the pressure range. All of the predicted values show close agreement at the lower pressure range and all within reasonable deviation across the entire range with the exception of the R-K equation of state. The fraction of total enthalpy that is represented by the departure portion is roughly 30% at its maximum level.

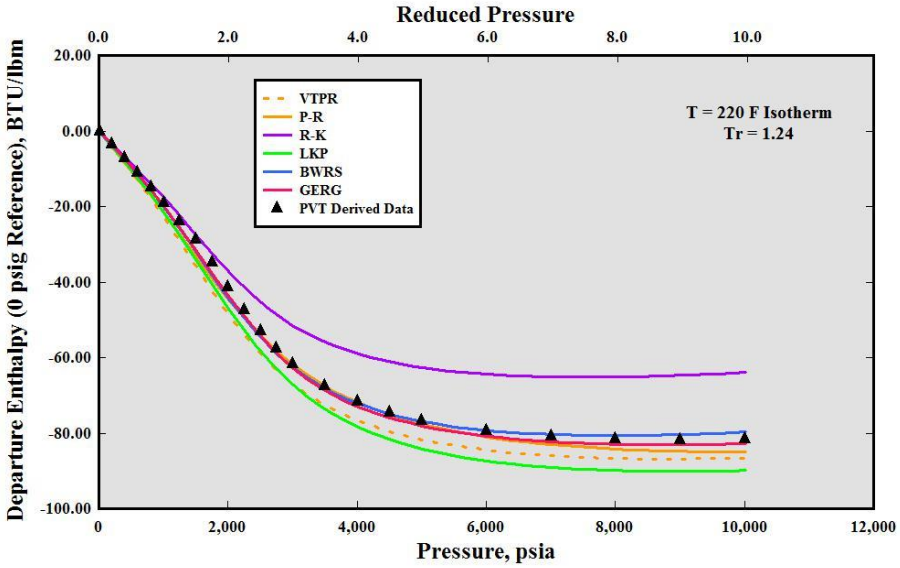

Figure 29: Departure Enthalpy for Carbon Dioxide / Ethane Mixture

Agreement between derived and predicted quantities of departure entropy is good in Figure 30 across the entire pressure range with the exception of the R-K equation of state.

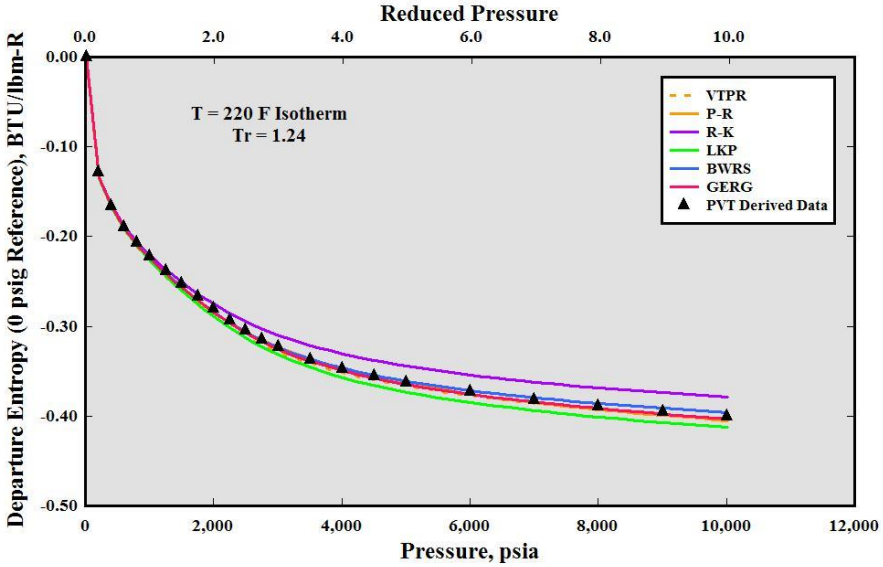

Figure 30: Departure Entropy for Carbon Dioxide / Ethane Mixture

The statistics for compressibility factor among all six isotherms is provided in Figure 31. Overall results are consistent with the other ethane / carbon dioxide mixture, however, deviations are higher for GERG, LKP and BWRS but still within a 2%

standard deviation. The remaining three equations of state exhibit higher deviations but the P-R and VTPR numbers are lower with the higher carbon dioxide concentration.

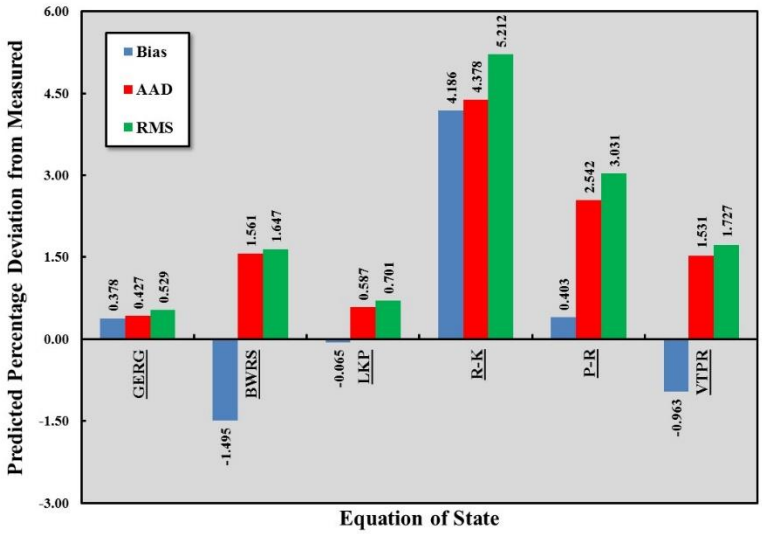

Figure 31: Compressibility Factor Percentage Deviations for Carbon Dioxide / Ethane Mixture

Sour Gas

Sour gas is typically composed of light paraffinic hydrocarbons with varying, but relatively small, amounts of hydrogen sulfide included. Given its toxic and potentially corrosive nature, the hydrogen sulfide will usually need to be separated from the total gas stream unless it is subject to reinjection. The physical properties of hydrogen sulfide are somewhat similar to carbon dioxide in that the critical pressure and temperature, Pc of 1305 psia (90 bara) and Tc of 212 F (100 C), are within common conditions experienced in industry. Although the acentric factor of hydrogen sulfide is less than that of carbon dioxide, it is a more polar molecule which can adversely affect property prediction by an equation of state.

Two different mixtures of methane and hydrogen sulfide will be evaluated herein with one being composed of 10% hydrogen sulfide on a mole fraction basis and the other a 30% concentration. The source of the PVT data is again from a publication by Reamer, et al. (1951). This paper contains a more extensive set of data than is utilized with higher portions of hydrogen sulfide, but the 30% maximum concentration was chosen due to known limits that are being reinjected at higher pressures.

90% Methane – 10% Hydrogen Sulfide Mixture

The first set of data to be examined will be the mixture containing 10% mole fraction of hydrogen sulfide. Six isotherms are included in this data set from 40 F to 340 F (4.4 C to 171 C) that represent reduced temperatures in a range from an approximate value of 1.33 to 2.13 and a reduced pressure ranging to a value above 13.0. Derived and predicted values of the compressibility in the vicinity of the center of the temperature range are compared in Figure 32.

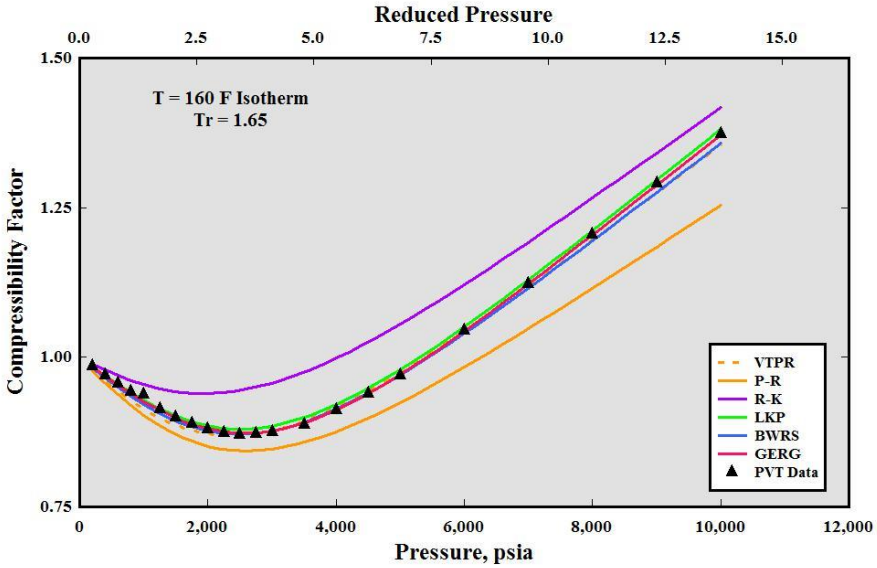

Figure 32: Compressibility Factor for 90% Methane / 10% Hydrogen Sulfide Mixture

A comparison of derived and predicted departure enthalpy for this gas mixture shows relatively close agreement with all equations of state with the exception of R-K and P-R. Given the maximum partial contribution of the departure enthalpy to total enthalpy is roughly 15%, the ability of the equations of state to accurately predict total enthalpy appears to be good. As has been previously noted, agreement between derived and predicted quantities is much closer at the lower pressures within the range.

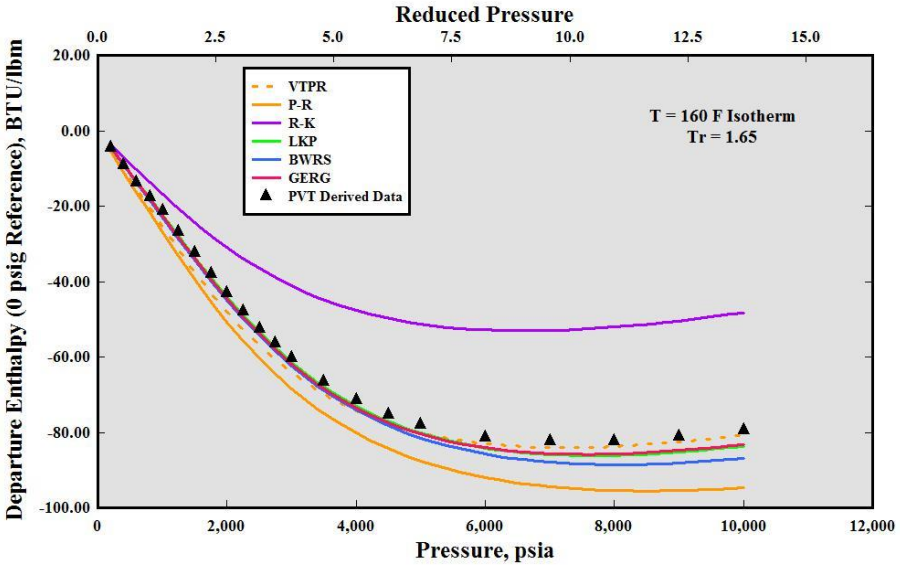

Figure 33: Departure Enthalpy for 90% Methane / 10% Hydrogen Sulfide Mixture

Predictions of departure entropy again show close proximity to each other and PVT data derived values. This is presented in Figure 34, where the largest deviation is attributed to the R-K equation of state.

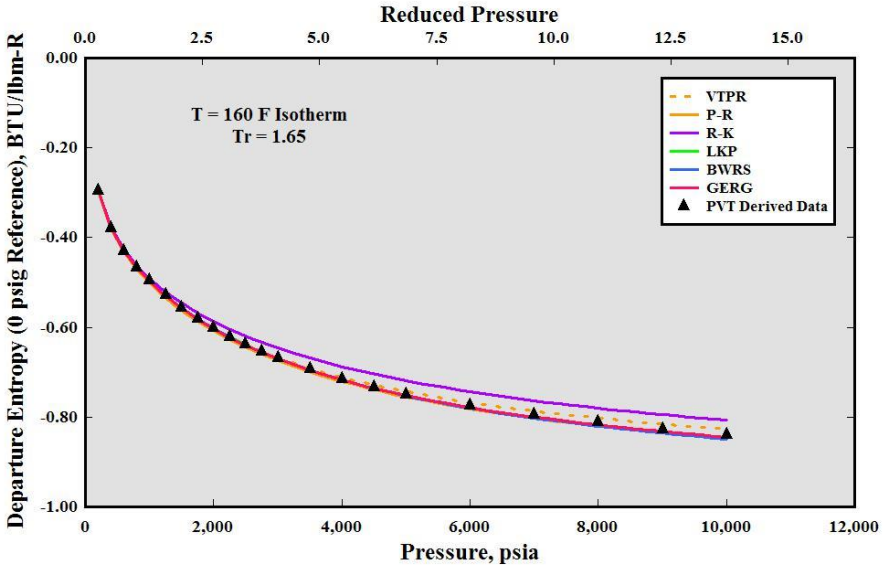

Figure 34: Departure Entropy for 90% Methane / 10% Hydrogen Sulfide Mixture

The percentage deviation statistics for the combined six isotherms are presented in Figure 35 below. Average errors and standard deviations within 1% are noted for four of the equations of state, although deviations for the R-K and P-R equations of state are above this limit. This behavior is consistent with the other gases examined thus far.

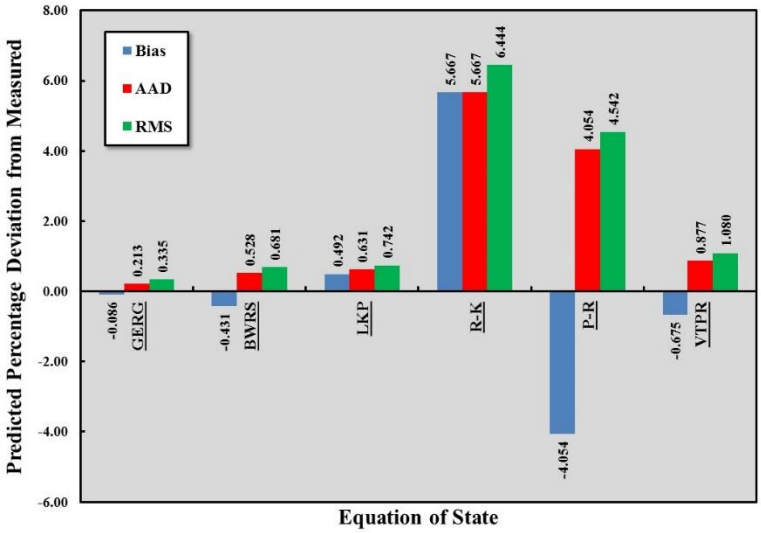

Figure 35: Compressibility Factor Deviations for 90% Methane / 10% Hydrogen Sulfide Mixture

70% Methane – 30% Hydrogen Sulfide Mixture

A larger concentration of 30% hydrogen sulfide is contained in the second mixture to be examined. This data set contains five equally spaced isotherms from 100 F to 340 F (37.8 C to 171 C), corresponding to a reduced temperature range of 1.27 to 1.81. Due to the increased amount of hydrogen sulfide with a higher critical pressure, the maximum reduced pressure is reduced to approximately 11.0.

The trend of compressibility factor is given in Figure 36. It is similar to that of the mixture with less hydrogen sulfide but with increased visible deviation with the LKP and VTPR equations of state in portions of the pressure range. The R-K and P-R equations of state display noticeable deviation across the entire range of pressures.

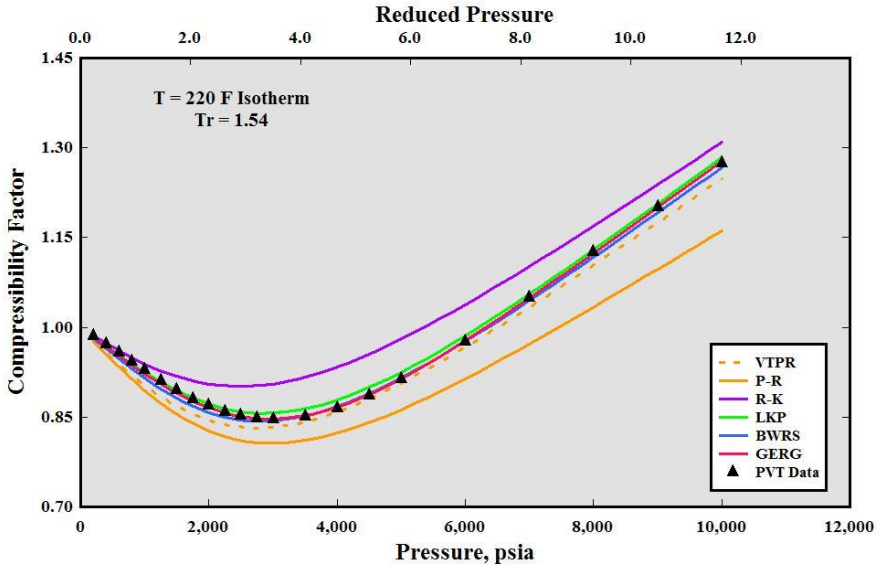

Figure 36: Compressibility Factor for 70% Methane / 30% Hydrogen Sulfide Mixture

Departure enthalpy reflects a similar trend and agreement between derived and predicted values. The maximum departure enthalpy magnitude as a proportion of total enthalpy is slightly greater, near 20%, for the higher hydrogen sulfide concentration. Predictions of departure enthalpy from the R-K and P-R equations of state display the greatest deviation.

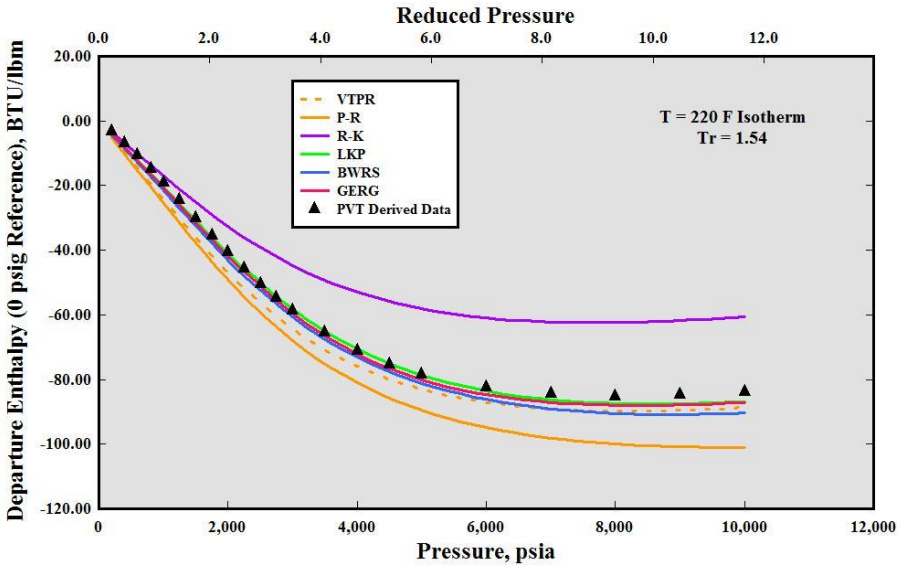

Figure 37: Departure Enthalpy for 70% Methane / 30% Hydrogen Sulfide Mixture

Comparable results for departure entropy are presented in Figure 38 below.

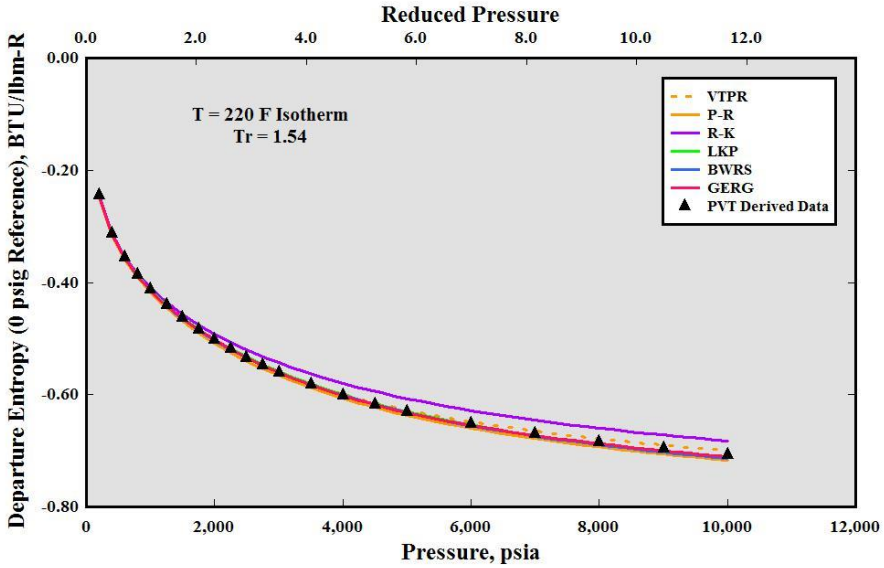

Figure 38: Departure Entropy for 70% Methane / 30% Hydrogen Sulfide Mixture

Summary statistics for the 30% hydrogen sulfide mixture for all isotherms are similar to the lower concentration mixture, but deviations are greater for all equations of state except R-K. This is expected given the higher proportion of the more complex and polar hydrogen sulfide molecule in the mixture. Average and standard deviations are still within 1% for GERG, LKP and BWRS, but larger for the other three relations.

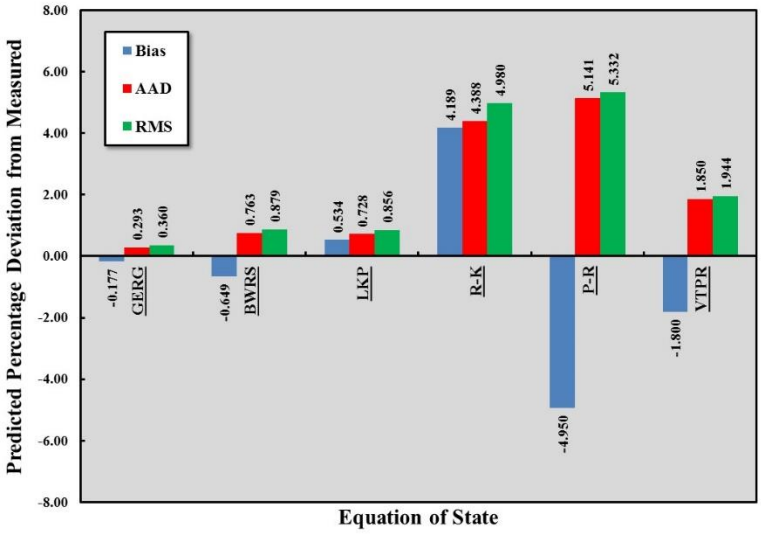

Figure 39: Compressibility Factor Deviations for 70% Methane / 30% Hydrogen Sulfide Mixture

Acid Gas

Acid gas is a mixture of primarily carbon dioxide and hydrogen sulfide in various proportions with small amounts of hydrocarbons potentially present. It is most commonly generated from gas sweetening processes where the acid gas components are removed from a hydrocarbon-rich stream and concentrated in a separation media regeneration operation. The significant toxic and corrosive properties of

acid gas render it difficult to handle in compression applications. The unique physical properties of both carbon dioxide and hydrogen sulfide can also complicate its behavior during compression. The critical pressures of carbon dioxide and hydrogen sulfide, 1070 psia (73.8 bara) and 1305 psia (90 bara), respectively, coupled with their relatively high critical temperatures, 88 F (31 C) and 212 F (100 C), respectively, result in their mixture pseudo-critical points being in the range of many industrial processes where they may exist. At pressures above their pseudo-critical points, they may be more easily handled with a pump design than a compressor if their temperatures can be controlled below their critical values due to their near constant density characteristics. Two acid gas compositions have been included due to their unique nature and potential compression application.

94% Carbon Dioxide – 6% Hydrogen Sulfide Mixture

The first acid gas mixture is composed of mostly carbon dioxide with a 94% mole fraction, leaving the hydrogen sulfide composition at nearly 6%. PVT data for this mixture was provided in the paper by Stouffer, et al. (2001). Maximum pressures available in this data set are more limited than the other data included in this study. The temperature range included is 125 F to 350F (51.7 C to 176.7 C) in four isotherms. This corresponds to a reduced temperature range of 1.05 to 1.46 with a maximum reduced pressure of 2.16.

A comparison of derived and predicted compressibility factors for this acid gas mixture is presented in Figure 40. It should be noted that there is good agreement with all equations of state in the lower half of the pressure range, with more deviation evident in the upper portion of the range. This is instructive in the fact that, regardless of gas mixture, at pressures below a reduced pressure of unity, deviations between the different equations of state is minimal in predicting thermophysical properties.

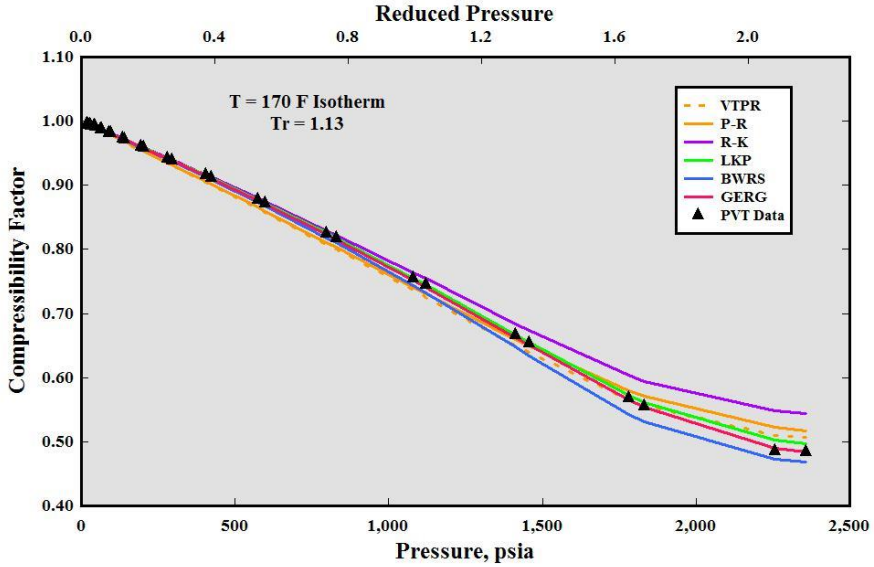

Figure 40: Compressibility Factor for Acid Gas 1 Mixture (94% CO2)

An examination of the departure enthalpy in Figure 41 shows comparable predicted values for all equations of state with the exception of R-K with notable deviations above 500 psia (34.5 bara). The deviation between predicted and derived values is more significant at the higher end of the pressure range. Given that the proportion of departure to total enthalpy at this maximum pressure is in the 30% to 40% range, the roughly 10% difference between predicted and derived departure enthalpy could result in a 3% to 4% difference in total enthalpy.

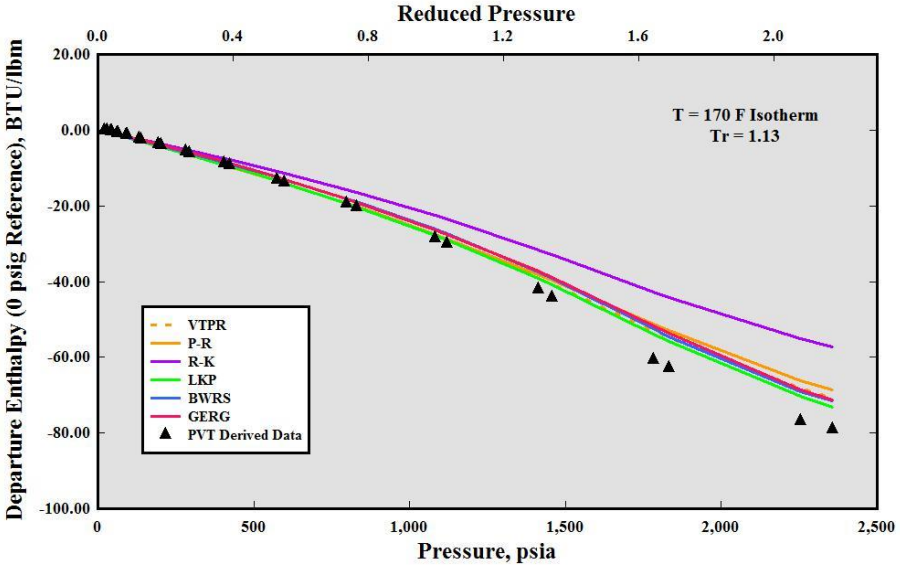

Figure 41: Departure Enthalpy for Acid Gas 1 Mixture (94% CO2)

Figure 42 displays good agreement between predicted and derived values of departure entropy across the entire range of the PVT data set. There appears to be some increased deviation with the R-K equation of state at the higher pressures, but this is not considered to be significant.

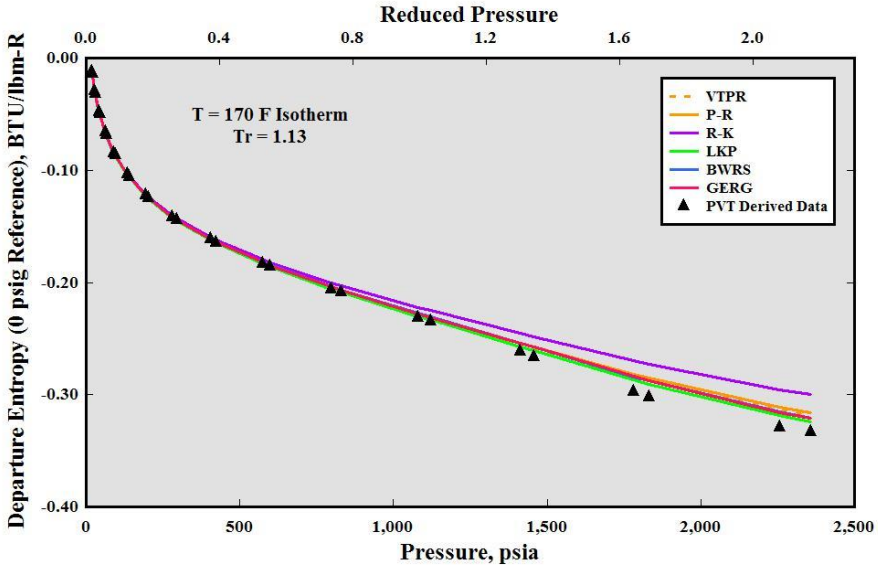

Figure 42: Departure Entropy for Acid Gas 1 Mixture (94% CO2)

It is evident from the summary statistics plot in Figure 43 that the deviations between the different equations of state are more even than has been presented for the other gases and gas mixtures. This may partially be due to the limited pressure range available in this data set and, possibly, the characteristics of this gas mixture. Standard deviations for the GERG and LKP equations of state are within 1%, whereas those related to BWRS and VTPR are within 2%.

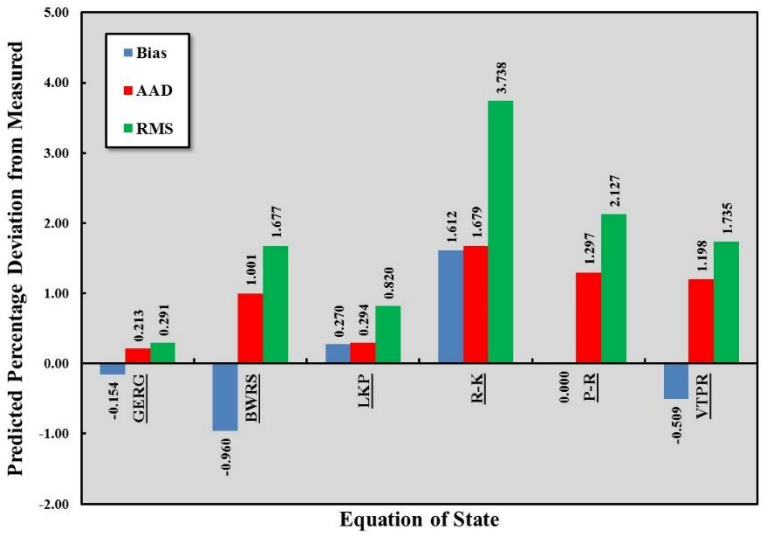

Figure 43: Compressibility Factor Deviations for Acid Gas 1 Mixture (94% CO2)

49% Carbon Dioxide – 51% Hydrogen Sulfide Mixture

A nearly equimolar mixture of carbon dioxide and hydrogen sulfide is represented in the second acid gas mixture. The PVT data set includes five isotherms with temperatures ranging from 125 F to 440 F (51.7 C to 226.7 C). This results in a reduced temperature range from 0.96 to 1.47 and an increased maximum reduced pressure of over 7.0. The data was found in part three of a six part technical article by Bailey, et al. (1987) that contained additional data on hydrogen sulfide and mixtures containing hydrogen sulfide.

Information for the compressibility factor is provided in Figure 44 for the 260 F (126.7 C) isotherm. Increased deviation among the various equations of state and between the experimentally derived values is evident, particularly near the compressibility factor minimum. P-R, LKP and GERG equations of state appear to be the most accurate predictors along this isotherm.

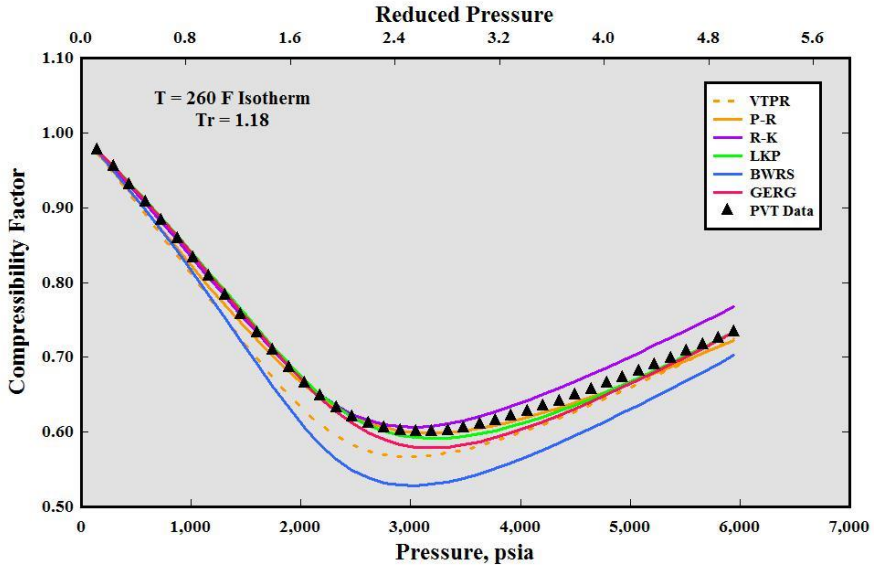

Figure 44: Compressibility Factor for Acid Gas 2 Mixture (49% CO2)

The departure enthalpy comparison is provided in Figure 45 for the second acid gas mixture. A questionable "bump" is obvious in the experimentally derived departure enthalpy between 1000 and 2000 psia (69 and 138 bara). It is believed to be due to its proximity to the top of the phase envelope, however additional evaluation may be warranted in the future. Beyond consideration of the "bump," closest agreement between the derived data and equation of state data is evident for the P-R, GERG and LKP equations of state. The remaining equations of state display greater deviation with R-K showing the most significant.

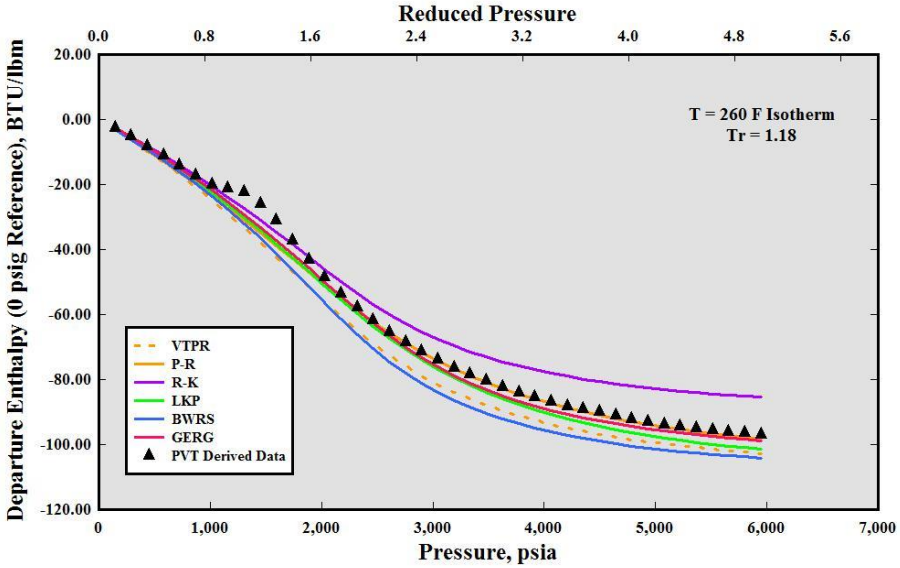

Figure 45: Departure Enthalpy for Acid Gas 2 Mixture (49% CO2)

With the exception of a comparable "bump" in the experimentally derived departure entropy in the same pressure range as the enthalpy, there is reasonably good agreement between the derived and predicted values. The R-K equation of state displays greater deviation in Figure 46 at the higher pressures as has also been noted previously.

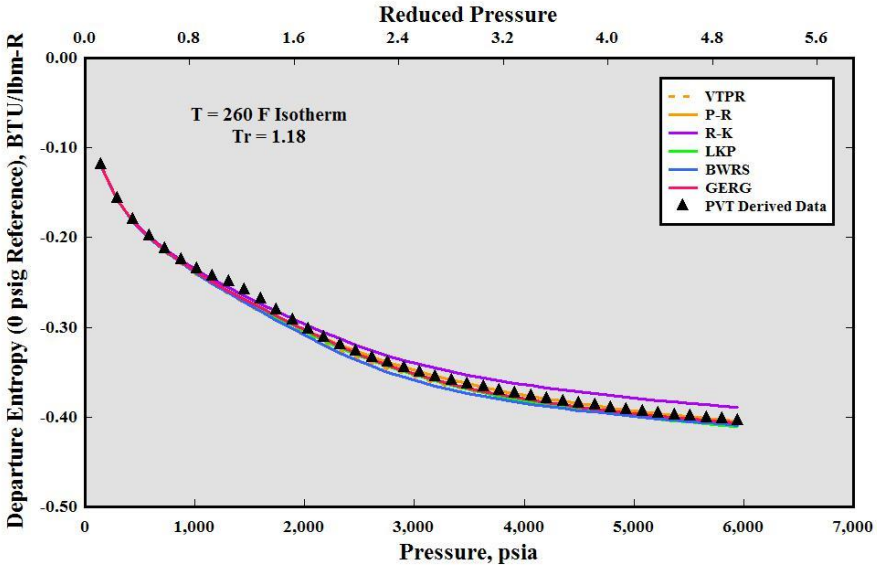

Figure 46: Departure Entropy for Acid Gas 2 Mixture (49% CO2)

The significant amount of hydrogen sulfide in the second acid gas composition results in a variation in the results of compressibility factor statistics. In this case, the P-R equation of state shows the smallest average and standard deviation differences across the entire temperature and pressure ranges, followed by GERG and LKP. The standard deviation of these three equations of state is less than 3%. The R-K, VTPR and BWRS equations of state showed significantly higher deviation with BWRS having the highest deviation.

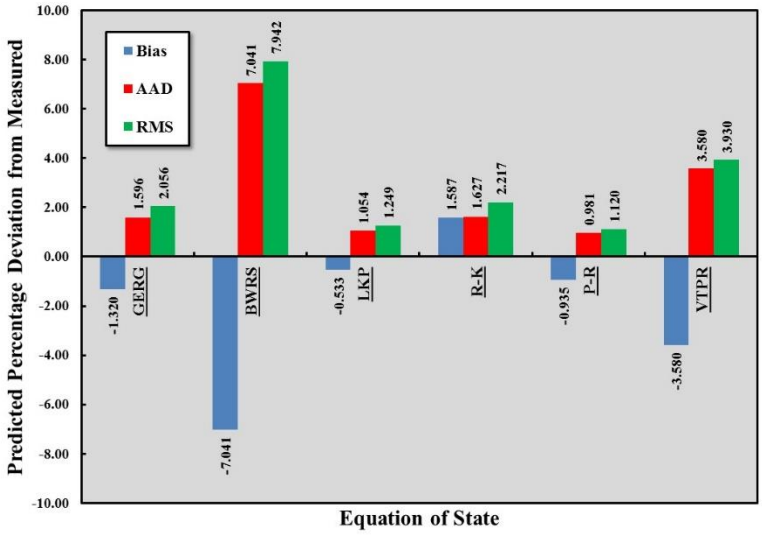

Figure 47: Compressibility Factor Deviations for Acid Gas 2 Mixture (49% CO2)

Summary

Although this investigation of different gases and gas mixtures cannot be considered exhaustive, it does represent a large class of industrially significant gases and represents a large amount of experimental PVT data. The data for the 11 gas mixtures included over

1000 separate data points distributed over 52 isotherms. Pressure ranges involved in many of the data sets extend beyond current compression technology application limits. The different gas mixtures included may also be utilized to estimate gas behavior and predict equation of state accuracy for comparable gas mixtures or gas physical property characteristics.

Thermophysical property prediction accuracy of each equation of state was provided for all of the gas mixtures included based upon the average and standard deviation of the compressibility factor. The relative rankings of the equations of state are provided below for each gas/gas mixture and an overall ranking based upon the summation of all gases examined. With only two exceptions, the relative ranking based upon absolute average deviation and root mean squared deviation were consistent, and the two that had deviations were minor and did not impact the overall ranking. The table below represents the average absolute deviation rankings.

Gas-Gas Mixture / EOS	GERG	BWRS	LKP	R-K	P-R	VTPR
Methane	1	2	4	5	6	3
Nitrogen	1	4	2	5	6	3
Carbon Dioxide	1	3	2	6	5	4
Sweet Natural Gas	1	2	3	6	5	4
Natural Gas	1	2	3	5	6	4
83% Ethane / 17% CO2	1	3	2	6	5	4
18% Ethane / 82% CO2	1	3	2	6	5	4
90% Methane / 10% H2S	1	2	3	6	5	4
70% Methane / 30% H2S	1	3	2	5	6	4
94% CO2 / 6% H2S	1	3	2	6	5	4
49% CO2 / 51% H2S	2	6	3	4	1	5
Overall Ranking	1	3	2	6	5	4

Table 1: Equation of State Accuracy Ranking

In addition to the evaluation of a specific equation of state to accurately predict the compressibility factor, predictions of departure enthalpy and entropy were also included based upon experimentally derived parameters calculated through cubic spline interpolations and numerical manipulation of the PVT data. Relevant statistical evaluation of the departure functions was not possible due to the fact that these departure functions in combination with their related ideal gas values provide total values and the proportion of departure to ideal quantities was not consistent between the different gases and gas mixtures involved. Additionally, extrapolation and calculation of the required parameters at the pressure and temperature extents of the data may be subject to error due to the characteristics of cubic splines. Nevertheless, predicted property deviations and the consistency of the general behavior of derived and predicted values across the involved pressure ranges lends credence to the ability of equations of state to estimate these values with relative accuracy based upon a given equation of state compressibility factor prediction accuracy.

COMPRESSION EXAMPLE COMPARISON

While the direct analysis of PVT data offers insight into how accurately any equation of state predicts the compressibility (or specific volume) of a gas or gas mixture, the addition of the derived departure enthalpy and entropy functions allows further insight into the ability of any equation of state to reasonably predict these additional thermodynamic functions, albeit at some increased level of uncertainty relative to the compressibility factor. This increased uncertainty may be due to inaccuracies introduced in fitting a spline function to the experimental PVT data and the numerical analysis required to obtain derivatives and integrals of the empirically-based compressibility factor functions.

Since all of these properties are utilized in calculating the required parameters describing compressor thermodynamic performance, additional inaccuracies resulting from the combination of these properties is possible and difficult to quantify. In order to better demonstrate this potential issue, a number of example applications have been evaluated to compare calculated compressor performance

parameters among the different equations of state included in this study. A baseline set of performance parameters has been established using the GERG equation of state with the other equation of state derived parameters being compared against these baseline values. The GERG equation of state was chosen due to its superior agreement with most of the gas mixtures included and the expectation that the accuracy of departure functions are likely related to compressibility factor estimate accuracy. All calculations were completed in accordance with the base Schultz method prescribed in ASME PTC 10 (1997).

Low Pressure Natural Gas

The first example application to be examined is that of the previously defined natural gas mixture including small amounts of nitrogen and carbon dioxide with the exact composition given in the paper by McLinden (2011) and identified as SNG-1. This represents a relatively low pressure example with suction pressure at 100 psig and suction temperature at 100 F. Discharge pressure and temperature are 300 psig and 260 F, respectively. Selected thermophysical properties and compressor performance parameters for each of the six equations of state are listed in the table below. Percentage deviations of critical compressor performance parameters relative to those calculated with REFPROP derived parameters are presented in the last four rows of the table.

Equation of State:	GERG	BWRS	LKP	R-K	P-R	VTPR
Suction Compressibility:	0.9853	0.9848	0.9857	0.9889	0.9815	0.9828
Suction Specific Volume (ft^3/lbm):	2.7982	2.7965	2.7990	2.8080	2.7869	2.7907
Discharge Compressibility:	0.9868	0.9851	0.9870	0.9946	0.9811	0.9839
Discharge Specific Volume (ft^3/lbm):	1.3134	1.3111	1.3135	1.3236	1.3056	1.3093
Polytropic Exponent:	1.3344	1.3324	1.3341	1.3420	1.3311	1.3337
Schultz Factor:	1.00195	1.00190	1.00140	1.00390	1.00140	0.99970
Polytropic Head (ft-lbf/lbm):	53180.2	53112.2	53161.0	53591.4	52886.5	52908.9
Polytropic Efficiency:	0.8253	0.8216	0.8218	0.8169	0.8245	0.8233
Work Input (ft-lbf/lbm):	64436.7	64643.4	64692.1	65600.9	64146.0	64261.5
Inlet Volumetric Flow Rate (acfm/MMSCFD):	94.4338	94.3786	94.4628	94.7667	94.0562	94.1816
Specific Power (ghp/MMSCFD):	65.90	66.11	66.16	67.09	65.60	65.72
Percentage Error Relative to REFPROP:						
Polytropic Head:	0.00	-0.13	-0.04	0.77	-0.55	-0.51
Polytropic Efficiency:	0.00	-0.45	-0.43	-1.02	-0.10	-0.24
Work Input:	0.00	0.32	0.40	1.81	-0.45	-0.27
Specific Power:	0.00	0.32	0.39	1.81	-0.45	-0.27

Table 2: Low Pressure "Typical" Natural Gas Compressor Performance Results

Comparison of these results demonstrates that with the exception of R-K, the results of all other equations of state agree within about 0.5%. This is primarily due to the fact that the specified suction and discharge conditions are nearly ideal where the differences between the equations of state are small. It should also be noted that many factory acceptance Type II tests are conducted with effectively inert gases at similar pressure and temperature conditions. This leads to the conclusion that performance calculations in the superheat region of the phase diagram at pressures below the critical pressure are likely to be relatively insensitive to the equation of state selected. Of course, the results from the R-K equation of state proves that this is not always the case.

Intermediate Pressure Natural Gas

As pressure levels are increased, operating conditions transition from the superheat region of the phase diagram into the dense phase region where the gases may begin to deviate more from ideal conditions. The gas mixture utilized in this hypothetical example are the same as the previous example. Suction pressure has been increased to 1000 psig while maintaining the suction temperature at 100 F. Discharge pressure is set at 3000 psig, keeping the compression ratio constant, while setting the discharge temperature at 300 F. Calculated parameters for this case are provided in Table 3 below.

Equation of State:	GERG	BWRS	LKP	R-K	P-R	VTPR
Suction Compressibility:	0.8784	0.8749	0.8802	0.9184	0.8573	0.8688
Suction Specific Volume (ft^3/lbm):	0.2820	0.2808	0.2825	0.2948	0.2751	0.2789
Discharge Compressibility:	0.9806	0.9818	0.9858	1.0412	0.9596	0.9849
Discharge Specific Volume (ft^3/lbm):	0.1438	0.1440	0.1446	0.1527	0.1407	0.1444
Polytropic Exponent:	1.6173	1.6298	1.6253	1.6552	1.6237	1.6549
Schultz Factor:	0.99047	0.98890	0.98940	1.01640	0.99110	0.97730
Polytropic Head (ft-lbf/lbm):	55096.5	54939.3	55234.0	59590.2	53870.8	54203.2
Polytropic Efficiency:	0.7228	0.7143	0.7189	0.6955	0.7118	0.7018
Work Input (ft-lbf/lbm):	76225.0	76911.4	76835.8	85674.8	75685.4	77239.4
Inlet Volumetric Flow Rate (acfm/MMSCFD):	9.5164	9.4777	9.5341	9.948	9.2859	9.4114
Specific Power (ghp/MMSCFD):	77.95	78.67	78.58	87.61	77.41	78.98
Percentage Error Relative to REFPROP:						
Polytropic Head:	0.00	-0.29	0.25	8.16	-2.22	-1.62
Polytropic Efficiency:	0.00	-1.18	-0.54	-3.78	-1.52	-2.91
Work Input:	0.00	0.90	0.80	12.40	-0.71	1.33
Specific Power:	0.00	0.92	0.80	12.39	-0.69	1.31

Table 3: Intermediate Pressure "Typical" Natural Gas Compressor Performance Results

Increased deviations in performance parameters are evident in this case. While predictions from BWRS and LKP are generally within about 1% of the assumed REFPROP (GERG) baseline, deviations represented by the R-K, P-R and VTPR equations of state tend to be larger. If reference is made to the compressibility factor plot of this gas in Figure 20, it is evident that the deviations in polytropic head follow deviations in the compressibility factors. The R-K equation of state significantly over-predicts the compressibility factor and polytropic head, while P-R consistently under-predicts the compressibility factor and polytropic head. Since the polytropic head is primarily dependent upon the derived specific volume (compressibility factor), this behavior is expected. Another observation that warrants attention is the value of the Schultz correction factor. Sandberg and Colby (2013) suggested that Schultz factor values of 1.00 +/- .01 represented the valid use of average polytropic exponents in the polytropic head calculations, but values beyond this tolerance range could result in unacceptable errors in the calculation. Some Schultz factor values in the above example fall outside of this range, signifying that an alternative calculation method to determine polytropic head may result in more accurate predictions.

The other three parameters are dependent upon accurate predictions of enthalpy and entropy which require accurate predictions of the departure functions. This becomes more difficult to predict due to the fact that departure values of enthalpy and entropy must be summed with the ideal gas values and then have total suction quantities subtracted from discharge conditions to determine work input, or specific enthalpy differential. Of course, efficiency is the ratio of polytropic head to work input, so the resulting values are sensitive to deviations in both compressibility factor and enthalpy differences. Finally, specific power is a function of the product of flow rate and work input, so it again is dependent upon the accuracy of predictions of both compressibility factor and enthalpies. Considering that relative deviations of all these parameters may vary differently across any specific pressure and temperature range, consistent prediction of the relative deviations in the calculated performance parameters may not be possible, however, overall trends of polytropic head do appear to correlate directly with predictions of compressibility factor.

High Pressure Natural Gas

A final example comparison calculation utilizing the natural gas mixture at significantly higher pressures is given below. In this case, the suction and discharge pressures were increased further. Suction conditions were set at 6000 psig and 100 F and discharge pressure and temperature were 9000 psig and 157 F, respectively. Although the pressure ratio is roughly half of the previous two examples, this case more accurately represents an actual selection due to the overriding factor of pressure differential versus pressure ratio. Operating conditions of this hypothetical example reach well into the dense phase region of the phase diagram.

Equation of State:	GERG	BWRS	LKP	R-K	P-R	VTPR
Suction Compressibility:	1.0618	1.0520	1.0595	1.1407	1.0000	1.0686
Suction Specific Volume (ft^3/lbm):	0.0575	0.0570	0.0574	0.0618	0.0541	0.0579
Discharge Compressibility:	1.3375	1.3248	1.3384	1.3961	1.2378	1.3312
Discharge Specific Volume (ft^3/lbm):	0.0532	0.0527	0.0533	0.0556	0.0493	0.0530
Polytropic Exponent:	5.2644	5.2454	5.4700	3.8321	4.2922	4.6012
Schultz Factor:	1.00006	0.99980	0.99940	1.04990	0.99940	0.96100
Polytropic Head (ft-lbf/lbm):	23850.4	23620.6	23815.6	26489.6	22238.9	22927.1
Polytropic Efficiency:	0.7155	0.7226	0.7117	0.7130	0.7092	0.6842
Work Input (ft-lbf/lbm):	33334.9	32687.6	33463.2	37151.0	31358.3	33509.8
Inlet Volumetric Flow Rate (acfm/MMSCFD):	1.9406	1.9227	1.9361	2.0845	1.8273	1.9528
Specific Power (ghp/MMSCFD):	34.09	33.41	34.20	37.97	32.10	34.25
Percentage Error Relative to REFPROP:						
Polytropic Head:	0.00	-0.96	-0.15	11.07	-6.76	-3.87
Polytropic Efficiency:	0.00	1.00	-0.53	-0.35	-0.88	-4.37
Work Input:	0.00	-1.94	0.38	11.45	-5.93	0.52
Specific Power:	0.00	-1.99	0.33	11.39	-5.85	0.46

Table 4: High Pressure "Typical" Natural Gas Compressor Performance Results

It is evident that the values of polytropic head correlate fairly well with the compressibility factors presented in Figure 20, but a comparison of work input deviations also follows the relative deviation of departure enthalpy provided in Figure 21. A reasonably consistent observation that exists is the deviation in efficiency for each equation of state is roughly equal to the deviation in polytropic head minus the deviation in work input. Another thing to be noted above is the amount of volume reduction (ratio of specific volumes) from suction to discharge conditions. The ratios in this example are approximately a value of 1.1 in comparison to the previous two examples with approximate ratios of 2. This ratio approaching unity represents a nearly constant density that exists well into the dense phase region where the fluid assumes properties of both gases and liquids.

Propane Refrigeration

The fourth of six examples to be evaluated represents a propane refrigeration application that might be the final section of a multi-section sideload compressor application. The discharge pressure is set as a result of condensing conditions of the propane against an ambient temperature related condenser. The assumed operating conditions of this compression application are a suction pressure and temperature of 100 psig and 86 F, along with discharge conditions of 220 psig and 147 F. The location of these conditions, particularly suction, on the phase diagram are in the superheat region, but closer to the saturated vapor boundary of the two-phase envelope than the natural gas example. The reduced temperatures are also lower, near or below a value of unity, with the net impact being lower values of compressibility factor.

Equation of State:	GERG	BWRS	LKP	R-K	P-R	VTPR
Suction Compressibility:	0.8660	0.8639	0.8630	0.8591	0.8637	0.8652
Suction Specific Volume (ft^3/lbm):	1.0027	1.0002	0.9990	0.9945	0.9999	1.0016
Discharge Compressibility:	0.7924	0.7911	0.7892	0.7870	0.7819	0.7848
Discharge Specific Volume (ft^3/lbm):	0.4985	0.4976	0.4964	0.4950	0.4918	0.4936
Polytropic Exponent:	1.0244	1.0256	1.0238	1.0262	1.0092	1.0118
Schultz Factor:	1.00503	1.00500	1.00450	1.02250	1.00500	1.00280
Polytropic Head (ft-lbf/lbm):	12019.8	11994.1	11966.2	12135.5	11921.6	11927.8
Polytropic Efficiency:	0.8714	0.8619	0.8736	0.8388	0.8710	0.8681
Work Input (ft-lbf/lbm):	13793.2	13915.9	13698.3	14468.1	13686.8	13740.1
Inlet Volumetric Flow Rate (acfm/MMSCFD):	80.9276	80.7246	80.6296	80.2657	80.6981	80.8405
Specific Power (ghp/MMSCFD):	33.73	34.03	33.50	35.38	33.47	33.61
Percentage Error Relative to REFPROP:						
Polytropic Head:	0.00	-0.21	-0.45	0.96	-0.82	-0.77
Polytropic Efficiency:	0.00	-1.09	0.25	-3.74	-0.05	-0.38
Work Input:	0.00	0.89	-0.69	4.89	-0.77	-0.38
Specific Power:	0.00	0.89	-0.69	4.89	-0.77	-0.38

Table 5: Propane Refrigeration Compressor Performance Results

Given that the reduced pressures involved in this application are well below unity, the gas behaves much like an ideal gas with small values of departure enthalpy and entropy relative to the ideal gas portion of total values. Accordingly, with the exception of R-K, deviations between property predictions among the different equations of state are within about 1%. This leads to the conclusion that although there are differences in deviations, most of the equations of state can adequately calculate the different performance parameters with acceptable accuracy.

High Pressure Sour Gas

A more challenging compression application is sour gas injection where the addition of the more complex hydrogen sulfide molecule may reduce accuracy from different equations of state. The case presented here approximates the Kashagan compressors mentioned in the introduction. The gas mixture was selected to be 80% methane and 20% hydrogen sulfide with suction conditions of 5500 psig and 120 F and discharge conditions of 9000 psig and 185 F.

Equation of State:	GERG	BWRS	LKP	R-K	P-R	VTPR
Suction Compressibility:	0.9418	0.9356	0.9464	1.0023	0.8754	0.9337
Suction Specific Volume (ft^3/lbm):	0.0541	0.0537	0.0543	0.0575	0.0502	0.0536
Discharge Compressibility:	1.2464	1.2353	1.2516	1.2883	1.1394	1.2252
Discharge Specific Volume (ft^3/lbm):	0.0487	0.0482	0.0489	0.0503	0.0445	0.0478
Polytropic Exponent:	4.6823	4.5821	4.6535	3.6636	4.0421	4.3285
Schultz Factor:	0.99973	0.99940	0.99890	1.06080	0.99930	0.96360
Polytropic Head (ft-lbf/lbm):	25750.2	25539.0	25842.2	28628.4	23712.1	24493.1
Polytropic Efficiency:	0.7969	0.8143	0.8055	0.7741	0.7865	0.7519
Work Input (ft-lbf/lbm):	32314.8	31362.0	32082.3	36981.7	30148.3	32573.8
Inlet Volumetric Flow Rate (acfm/MMSCFD):	1.9445	1.9315	1.9536	2.0692	1.8071	1.9275
Specific Power (ghp/MMSCFD):	35.22	34.18	34.98	40.33	32.89	35.50
Percentage Error Relative to REFPROP:						
Polytropic Head:	0.00	-0.82	0.36	11.18	-7.91	-4.88
Polytropic Efficiency:	0.00	2.19	1.08	-2.86	-1.30	-5.64
Work Input:	0.00	-2.95	-0.72	14.44	-6.70	0.80
Specific Power:	0.00	-2.94	-0.69	14.51	-6.62	0.79

Table 6: Sour Gas Reinjection Compressor Performance Results

Results for the sour gas application example follow the compressibility factor deviation results for all equations of state except for BWRS and VTPR. In this case, the predicted polytropic head continues to agree with the compressibility factor deviations, but work input deviation for BWRS exceeds that of VTPR due to greater departure enthalpy deviation in the applicable pressure range. The net result is that BWRS provides a more accurate prediction of polytropic head, but less accurate than VTPR for work input and specific power. LKP provides the closest prediction to the GERG baseline, and R-K and P-R provide the largest positive and negative deviations for both head and work input, respectively.

Intermediate Pressure Acid Gas

The final and potentially most difficult application to evaluate within the scope of this investigation is an acid gas compression case. Due to the current practice of pumping the fluid at pressures above the critical point, the discharge pressure has been limited to 1000 psig. The handled gas is composed of a 50%/50% mixture of carbon dioxide and hydrogen sulfide. The operating conditions have been set to 300 psig and 100 F at suction and 1000 psig and 325 F at discharge. Results of the performance parameter calculations are given in Table 7.

Equation of State:	GERG	BWRS	LKP	R-K	P-R	VTPR
Suction Compressibility:	0.8802	0.8690	0.8792	0.8651	0.8713	0.8736
Suction Specific Volume (ft^3/lbm):	0.4303	0.4248	0.4297	0.4228	0.4258	0.4270
Discharge Compressibility:	0.8870	0.8679	0.8904	0.8879	0.8712	0.8766
Discharge Specific Volume (ft^3/lbm):	0.1885	0.1845	0.1892	0.1887	0.1852	0.1863
Polytropic Exponent:	1.4187	1.4036	1.4275	1.4510	1.4056	1.4116
Schultz Factor:	0.99954	1.00070	0.99890	1.02620	0.99800	0.99490
Polytropic Head (ft-lbf/lbm):	27254.3	26811.6	27275.3	27765.7	26822.5	26861.4
Polytropic Efficiency:	0.7674	0.7566	0.7653	0.7551	0.7944	0.7916
Work Input (ft-lbf/lbm):	35516.5	35437.7	35638.0	36769.8	33764.2	33931.2
Inlet Volumetric Flow Rate (acfm/MMSCFD):	30.7481	30.3526	30.7082	30.2159	30.4301	30.5127
Specific Power (ghp/MMSCFD):	76.91	76.73	77.18	79.63	73.12	73.48
Percentage Error Relative to REFPROP:						
Polytropic Head:	0.00	-1.62	0.08	1.88	-1.58	-1.44
Polytropic Efficiency:	0.00	-1.40	-0.27	-1.60	3.52	3.16
Work Input:	0.00	-0.22	0.34	3.53	-4.93	-4.46
Specific Power:	0.00	-0.24	0.35	3.54	-4.93	-4.47

Table 7: Acid Gas Reinjection Compressor Performance Results

Results show a significant difference in polytropic head deviation between that predicted by P-R, LKP and GERG, which is not consistent with the statistical results in Figure 47. Further inspection of the compressibility factor for the similar gas evaluated in Figure 44 reveals much closer agreement between the different equations of state below 1000 psia and increased deviation above this pressure level with better correlation attributed to P-R, LKP and GERG equations of state. An additional examination of a more limited range of the PVT data below 1000 psig reveals different results with the R-K equation of state actually showing the lowest deviation between predicted and experimental PVT data, followed by GERG and LKP. Utilizing this information and changing the baseline performance parameters from REFPROP to R-K yields the modified deviation comparison in Table 8.

Percentage Error Relative to R-K:	GERG	BWRS	LKP	R-K	P-R	VTPR
Polytropic Head:	-1.84	-3.44	-1.77	0.00	-3.40	-3.26
Polytropic Efficiency:	1.62	0.20	1.35	0.00	5.20	4.83
Work Input:	-3.41	-3.62	-3.08	0.00	-8.17	-7.72
Specific Power:	-3.41	-3.65	-3.08	0.00	-8.18	-7.73

Table 8: Acid Gas Reinjection Alternate Performance Comparison

These revised performance parameter deviations compare more favorably to the more limited pressure range compressibility factor deviations and the relative agreement between derived departure enthalpy and work input deviations. This challenging example illustrates the potential need to focus on a reduced pressure range to ensure more accurate analysis if there is significant difference and variation in equation of state accuracy across the entire range of evaluated pressures in a PVT data set. Determination of such variance may require an analysis of predicted versus empirical deviation of compressibility factor among the evaluated equations of state across the pressure range of interest.

Notwithstanding the above analysis of possible variation in equation of state accuracy across a data set range, Table 8 also reveals a more consistent and substantial deviation between the baseline and remaining equation of state performance parameter predictions. This serves to further illustrate the more challenging task of thermodynamic property prediction represented by the acid gas case even at relatively low pressures where the deviations were much smaller between most of the equations of state.

CONCLUSIONS

This more comprehensive evaluation of equation of state impacts on compressor performance has not only validated conclusions of the previous investigation, but also expanded overall understanding of this topic that allows greater confidence in the determination of critical thermodynamic operating parameters such as polytropic head, efficiency and absorbed power for a specific set of compression operating conditions. Specifically, this effort has:

- Provided deviation magnitudes between experimentally obtained compressibility factors and several available equations of state for a selected number of single component gases and gas mixtures intended to represent a broad cross-section of industrially significant gases and range of compression applications. These compressibility factor deviations were further utilized to correlate deviations in calculated polytropic head between the included equations of state for a number of representative compressor services.
- Demonstrated that although magnitudes of empirically derived departure enthalpy and entropy show varying deviations with predicted values, comparison of overall behavior trends and agreement with predictions of total enthalpy and entropy confirms the relative ability among the different equations of state to supply accurate estimations of these thermodynamic properties for a specific gas mixture and operating conditions. In general, the accuracy of departure values of enthalpy and entropy appear to be correlated to compressibility factor accuracy.
- Further justified the advisability and need for the User and Equipment Supplier to mutually agree on the choice of equation of state to be used for performance prediction, acceptance testing (if applicable), analyses of “as tested” performance, and field performance evaluation and monitoring to ensure the most accurate calculation of compressor performance possible. This agreement should be articulated prior to submittal of final predicted performance and equipment contract award. Recognition of operating and acceptance testing pressure range and gas behavior need to be included for testing and design considerations.
- Established the necessity of obtaining experimental PVT data and completing additional analyses for challenging or novel gases and gas mixtures or unique operating conditions to allow the most accurate determination of compressor performance parameters. It is also recognized that proper selection of thermodynamic models and calculation methods which are beyond the scope of this paper can also have a significant impact on accuracy and should be selected intelligently.

NOMENCLATURE

P = Pressure
Pc = Critical pressure for single component gases, Pseudo-critical pressure for gas mixtures
Pr = Reduced pressure, P/Pc
v = Specific volume
V = Volume
T = Temperature
Tc = Critical temperature for single component gases, Pseudo-critical temperature for gas mixtures

Tr = Reduced temperature, T/Tc
R = Universal gas constant
MW = Gas molecular weight
Z = Compressibility factor
n = Polytropic exponent
Wp = Polytropic head (work)
ηp = Polytropic efficiency
Wis = Isentropic head (work)
ηis = Isentropic efficiency
f_s = Schultz correction factor
h = Specific enthalpy
H = Total enthalpy
s = Specific entropy
S = Total entropy
ṁ = Mass flow rate
PWR = Compressor section absorbed gas power
U = Impeller tip speed (Appendix A), Total internal energy (Appendix B)
Cp_0 = Constant pressure specific heat
μp = Polytropic head coefficient, dimensionless
μis = Isentropic head coefficient, dimensionless
Cx = Equation unit conversion constants (x is number) as defined below

Subscripts

s = Suction conditions
d = Discharge conditions
di = Isentropic path discharge conditions
is = Isentropic
p = Polytropic
ideal = Ideal gas property
real = Real gas property
departure = Departure property

Equation Unit Conversion Constants

Equation Unit Conversion Constants	Imperial Units	SI Units
Equation Parameter Units	P_s, P_d in psia v_s, v_d in ft^3/lbm T_s, T_d in R *Wp*, *Wis* in ft*lbf/lbm h_s, h_d in BTU/lbm *ṁ* in lbm/min *PWR* in hp *U* in ft/sec	P_s, P_d in bara v_s, v_d in m^3/kg T_s, T_d in K *Wp*, *Wis* in J/kg h_s, h_d in J/kg *ṁ* in kg/hr *PWR* in kW *U* in m/sec
C1	144.00	100,000.00
C2	1545.349	8314.472
C3	778.169	1.000
C4	3.0303 x 10^{-5}	2.7778 x 10^{-7}
C5	2.3581 x 10^{-2}	2.7778 x 10^{-7}

APPENDIX A – ASME PTC 10 Equations

The governing industry standard for determining centrifugal compressor performance, particularly in the United States, is ASME PTC 10 – 1997, "Performance Test Code on Compressors and Exhausters." The ISO equivalent of this standard is ISO 5389 with essentially the same equations and calculation methodology. ASME PTC 10 defines the minimum requirements for compressor testing including setup and instrumentation, computation of results, and uncertainty analysis. It is applicable for both inert gas, Type 2 tests such as might be encountered in a factory testing program and full load testing according to Type 1 requirements that might be applied to factory full load testing or field testing.

Compressor performance is obtained through the measurement of a limited number of readily available operating parameters. Total (stagnation) pressure and temperature at both suction and discharge conditions are required along with the compressor operating speed. The flow rate is determined by some type of flow meter which typically uses temperature, static pressure and differential pressure measurement at the meter. Gas composition and barometric pressure are also required. Once these parameters have been determined, the following physical and thermodynamic parameters can be derived and compressor performance established. There are two popular thermodynamic models that are used to describe compressor performance, the isentropic process and the polytropic process. Although simpler to manipulate, the isentropic process is more limited in application due to its restriction to an initially defined pressure ratio. The polytropic process can be used more accurately across varying compression ratios with greater accuracy. A majority of process compression equipment suppliers currently use the polytropic relations.

Regardless of thermodynamic model used, isentropic discharge conditions must be estimated and used in a number of the calculations. These isentropic discharge conditions are determined by setting the discharge pressure equal to the actual discharge pressure and varying the temperature to achieve the calculated entropy constant with the suction conditions. This is typically an iterative calculation utilizing relations derived from an equation of state.

The various parameters that may be calculated are:

Isentropic exponent:

$$n_{is} = \ln(\frac{P_d}{P_s}) \Big/ \ln(\frac{v_s}{v_{di}})$$

Schultz Correction Factor:

$$f_s = \frac{(h_{di} - h_s)}{\left(\frac{n_{is}}{n_{is}-1}\right)(P_d * v_{di} - P_s * v_s)} * \frac{C3}{C1}$$

Isentropic Head:

$$Wis = (h_{di} - h_s) * C3 = C1 * \left(\frac{n_{is}}{n_{is}-1}\right) * f_s * P_s * v_s \left[\left(\frac{P_d}{P_s}\right)^{(n_{is}-1)/n_{is}} - 1\right]$$

Isentropic Head Coefficient:

$$\mu_{is} = \frac{g_c * Wis}{\sum U^2}$$

Isentropic Efficiency:

$$\eta_{is} = \frac{(h_{di} - h_s)}{(h_d - h_s)} = \frac{Wis}{C3 * (h_d - h_s)}$$

Polytropic Exponent:

$$n_p = \ln(\frac{P_d}{P_s}) \Big/ \ln(\frac{v_s}{v_d})$$

Polytropic Head:

$$Wp = C1 * \left(\frac{n_p}{n_p - 1}\right) * f_s * P_s * v_s \left[\left(\frac{P_d}{P_s}\right)^{(n_p - 1)/n_p} - 1\right]$$

Polytropic Head Coefficient:

$$\mu_p = \frac{g_c * Wp}{\sum U^2}$$

Polytropic Efficiency:

$$\eta_p = \frac{Wp}{C3 * (h_d - h_s)}$$

Gas Horsepower:

$$PWR = \frac{C4 * \dot{m} * Wis}{\eta_{is}} = \frac{C4 * \dot{m} * Wp}{\eta_p}$$

APPENDIX B – Derivation of Real Gas Departure Functions

Real gas thermodynamic properties such as enthalpy and entropy can be derived from ideal relation for such parameters as the isobaric specific heat capacity and an equation of state that provides a relation for the compressibility. Taking enthalpy as an example and assuming that the enthalpy is a function of both temperature and pressure:

$$H = H(T, P)$$

The enthalpy is also defined as:

$$H = U + PV$$

with its derivative being:

$$dH = dU + d(PV) = dU + PdV + VdP$$

Reference to any number of thermodynamics texts will also show that the derivative of the internal energy can be defined as:

$$dU = TdS - PdV$$

Combining the above two relations yields:

$$dH = TdS + VdP$$

Along an isotherm, this may be expressed as:

$$\left(\frac{\partial H}{\partial P}\right)_T = T\left(\frac{\partial S}{\partial P}\right)_T + V$$

Again, reference to any thermodynamics text will show that the Maxwell relations give:

$$\left(\frac{\partial S}{\partial P}\right)_T = -\left(\frac{\partial V}{\partial T}\right)_P$$

Substitution results in the following relation:

$$\left(\frac{\partial H}{\partial P}\right)_T = \left[V - T\left(\frac{\partial V}{\partial T}\right)_P\right]$$

Next, taking the total derivative of the enthalpy yields:

$$dH = \left(\frac{\partial H}{\partial T}\right)_P dT + \left(\frac{\partial H}{\partial P}\right)_T dP$$

but, by definition, the isobaric specific heat capacity is defined as:

$$Cp_0 = \left(\frac{\partial H}{\partial T}\right)_P$$

Substitution of both of these terms into the enthalpy total derivative yields:

$$dH = Cp_0 dT + \left[V - T\left(\frac{\partial V}{\partial T}\right)_P\right] dP$$

For an ideal gas, PV = RT, the second term is found to be equal to zero:

$$\left[V - T\left(\frac{\partial V}{\partial T}\right)_P\right]_{ideal} = 0$$

This simplifies the relation for enthalpy to the familiar form:

$$dH = Cp_0 dT$$

However, for a real gas, PV = ZRT, the second term is not equal to zero. This term is often referred to as the residual or departure function. It is related to the derivative of the compressibility and thus may be determined from an equation of state.

$$\left[V - T\left(\frac{\partial V}{\partial T}\right)_P\right]_{real} = \frac{-RT^2}{P}\left(\frac{\partial Z}{\partial T}\right)_P$$

This results in the more general form of enthalpy for a real gas which is shown to be a function of both pressure and temperature. Integration of this equation to determine a change in enthalpy between two states is then accomplished along an isobar for the first term and then an isotherm for the second term.

$$dH = Cp_0 dT - \frac{RT^2}{P}\left(\frac{\partial Z}{\partial T}\right)_P dP$$

Finally, the total change in enthalpy between two state points is given by:

$$\Delta H = \int Cp_0 dT - \int \frac{RT^2}{P}\left(\frac{\partial Z}{\partial T}\right)_P dP$$

A similar analysis for the entropy can be derived that results in the following relationships for the total derivative of entropy given that it is a function of temperature and pressure:

$$dS = \frac{Cp_0}{T} dT - \left(\frac{\partial V}{\partial T}\right)_P dP$$

Which, for an ideal gas reduces to:

$$dS = \frac{Cp_0}{T} dT - \frac{R}{P} dP$$

and, for a real gas:

$$dS = \frac{Cp_0}{T} dT - \left[\frac{ZR}{P} + \frac{RT}{P}\left(\frac{\partial Z}{\partial T}\right)_P\right] dP$$

Finally, integrating to obtain the entropy difference between two state points:

$$\Delta S = \int \frac{Cp_0}{T} dT - \int \left[\frac{ZR}{P} + \frac{RT}{P} \left(\frac{\partial Z}{\partial T} \right)_P \right] dP$$

Once again, the residual function is demonstrated to be a function of the compressibility which can be derived directly from an equation of state. The integration of both equations to determine the change in enthalpy and entropy is accomplished by isobarically integrating the temperature dependent first term and isothermally integrating the pressure dependent second term.

REFERENCES

ASME PTC 10-1997, "Performance Test Code on Compressors and Exhausters," The American Society of Mechanical Engineers, New York, New York.

Atilhan, M., Aparicio, S., Ejaz, S., Cristancho, D., and Hall, K. R., 2011, "PρT Behavior of a Lean Synthetic Natural Gas Mixture Using Magnetic Suspension Densimeters and an Isochoric Apparatus: Part I," American Chemical Society, Journal of Chemical Engineering Data, Vol. 56, pp. 212–221.

Atilhan, M., Aparicio, S., Ejaz, S., Cristancho, D., Mantilla, I., and Hall, K. R., 2011, "Accurate P-ρ-T Behavior of Three Lean Synthetic Natural Gas Mixtures Using a Magnetic Suspension Densimeter and Isochoric Apparatus from (250 to 450) K with Pressures up to 150 MPa: Part II," American Chemical Society, Journal of Chemical Engineering Data, Vol. 56, pp. 3766–3774.

Bailey, D. M., Liu, C. -H., Holste, J. C., Eubank, P. T. and Hall, K. R., January 1987, "Energy Functions for H2S: Part 3 – Near-Equimolar Mixture with CO2," *Hydrocarbon Processing,* Vol. 66, No. 1, pp. 73–74.

Cristancho, D. E., Mantilla, I. D., Ejaz, S., Hall, K. R., Atilhan, M., and Iglesia-Silva, G. A., 2010, "Accurate PρT Data for Methane from (300 to 450) K up to 180 MPa," American Chemical Society, Journal of Chemical Engineering Data, Vol. 55, pp. 826–829.

Cristancho, D. E., Mantilla, I. D., Coy, A., Tibaduiza, A., Ortiz-Vega, D. O., Hall, K. R., and Iglesia-Silva, G. A., 2011, "Accurate P-ρ-T Data and Phase Boundary Determination for a Synthetic Residual Natural Gas Mixture," American Chemical Society, Journal of Chemical Engineering Data, Vol. 56, pp. 826–832.

Jhaveri, B. S. and Youngren, G. K., 1988, "Three-Parameter Modification of the Peng-Robinson Equation of State to Improve Volumetric Predictions," SPE Reservoir Engineering, pp. 1033–1040.

Kunz, O. and Wagner, W., October 2012, "The GERG-2008 Wide-Range Equation of State for Natural Gases and Other Mixtures: An Expansion of GERG-2004," ACS Publications, Journal of Chemical and Engineering Data, Vol. 57, No. 11, pp. 3032-3091.

Lemmon, E.W., Huber, M.L., and McLinden, M.O., 2010, *NIST Standard Reference Database 23: Reference Fluid Thermodynamic and Transport Properties-REFPROP*, Version 9.0, National Institute of Standards and Technology, Standard Reference Data Program, Gaithersburg, MD.

Lin, C. –J. and Hopke, S. W., 1974, "Application of the BWRS Equation to Methane, Ethane, Propane, and Nitrogen Systems," AIChE Chemical Engineering Progress Symposium Series, Vol. 70, No. 140.

Mantilla, I. D., Cristancho, D. E., Ejaz, S., Hall, K. R., Atilhan, M., and Iglesia-Silva, G. A., 2010, "New P-ρ-T Data for Nitrogen at Temperatures from (265 to 400) K at Pressures up to 150 MPa," American Chemical Society, Journal of Chemical Engineering Data, Vol. 55, pp. 4227–4230.

Mantilla, I. D., Cristancho, D. E., Ejaz, S., Hall, K. R., Atilhan, M., and Iglesia-Silva, G. A., 2010, "P-ρ-T Data for Carbon Dioxide from (310 to 450) K up to 160 MPa," American Chemical Society, Journal of Chemical Engineering Data, Vol. 55, pp. 4611–4613.

McLinden, M. O., 2011, "P-ρ-T Behavior of Four Lean Synthetic Natural-Gas-Like Mixtures from 250 K to 450 K with Pressures to 37 MPa," American Chemical Society, Journal of Chemical Engineering Data, Vol. 56, pp. 606–613.

Peng, D. –Y. and Robinson, D. B., 1976, "A New Two-Constant Equation of State," American Chemical Society, Industrial Engineering Chemical Process Design and Development, Vol. 15, No.1.

Plocker, U., Knapp, H. and Prausnitz, J., 1978, "Calculation of High-Pressure Vapor-Liquid Equilibria from a Corresponding-States Correlation with Emphasis on Asymmetric Mixtures," American Chemical Society, Industrial Engineering Chemical Process Design and Development, Vol. 17, No.3.

Reamer, H. H., Olds, R. H., Sage, B. H., and Lacey, W. N., 1945, "Phase Equilibria in Hydrocarbon Systems: Volumetric Behavior of Ethane-Carbon Dioxide System," American Chemical Society, Industrial and Engineering Chemistry, Vol. 37, No. 7, pp. 688 - 691.

Reamer, H. H., Sage, B. H., and Lacey, W. N., 1951, "Phase Equilibria in Hydrocarbon Systems: Volumetric and Phase Behavior of the Methane-Hydrogen Sulfide System," American Chemical Society, Industrial and Engineering Chemistry, Vol. 43, No. 4, pp. 976 - 981.

Redlich, O. and Kwong, J. N. S., 1949, "On the Thermodynamics of Solutions V: An Equation of State. Fugacities of Gaseous Solutions," Chemical Review, Vol. 44, No. 1, pp. 233 – 244.

Sandberg, M. R., 2005, "Equation of State Influences on Compressor Performance Determination," Proceedings of the 34th Turbomachinery Symposium, Turbomachinery Laboratory, Texas A&M University, College Station, Texas, pp. 121-129.

Sandberg, M. R. and Colby, G. M., 2013, "Limitations of ASME PTC 10 in Accurately Evaluating Centrifugal Compressor Thermodynamic Performance," Proceedings of the 42nd Turbomachinery Symposium, Turbomachinery Laboratory, Texas A&M University, College Station, Texas.

Stouffer, C. E., Kellerman, S. J., Hall, K. R., Holste, J. C., Gammon, B. E., and Marsh, K. N., 2001, "Densities of Carbon Dioxide + Hydrogen Sulfide Mixtures from 220 K to 450 K at Pressures up to 25 MPa," American Chemical Society, Journal of Chemical Engineering Data, Vol. 46, pp. 1309–1318.

BIBLIOGRAPHY

De Boor, C., 1978, *A Practical Guide to Splines*, New York, New York, Springer-Verlag.

Edmister, W. C. and Lee, B. I., 1984, *Applied Hydrocarbon Thermodynamics, Volume 1, Second Edition*, Houston, Texas, Gulf Publishing Company.

Knott, G. D., 2000, *Interpolating Cubic Splines*, Boston, Massachusetts, Birkhäuser.

Lüdtke, K. H., 2004, *Process Centrifugal Compressors: Basics, Function, Operation, Design, Application*, Berlin, Germany, Springer-Verlag.

Reid, R. C., Prausnitz, J. M. and Sherwood, T. K., 1977, *The Properties of Gases and Liquids, Third Edition*, New York, New York, McGraw-Hill Book Company.

Reid, R. C., Prausnitz, J. M. and Poling, B. E., 1987, *The Properties of Gases and Liquids, Fourth Edition*, New York, New York, McGraw-Hill Book Company.

Wark, K., 1995, *Advanced Thermodynamics for Engineers*, New York, New York, McGraw-Hill, Incorporated.

ACKNOWLEDGEMENTS

The author would like to acknowledge the valuable insight and discussions with Professor James C. Holste of the Artie McFerrin Department of Chemical Engineering at Texas A&M University regarding the subject matter of experimental measurement of PVT properties and evaluation of thermophysical parameters.